represent a microengineering platform that more closely mimics *in vivo* microvascular organization. Indeed, endothelial cells are in most of the cases just the inner layer of a more complex blood vessel multi-stratum organization, which consists of smooth muscle cells, ECM and fibroblasts. Many mechanical and biological functions rely on this architecture that if recapitulated, would be crucial to the generation of a new class of *in vitro* engineered vascular structures. By encapsulating tissue specific cell populations in the outer hydrogel compartment, the proposed combination can be scaled to the generation of multicellular vascularized 3D organoids (such as hepatic lobules and bone osteons). This approach could also prospectively take advantage of spatially specific designs of hydrogel for each layer/compartment (e.g. localized biochemical signals or mechanical characteristic).

4. Conclusions

In this study a combination of SAM-based cell deposition and hydrogel photocrosslinking was proposed as a platform for engineering 3D tissue constructs, and specifically applied to the generation of hollow vascular structures. The cell deposition process was found to rely on two distinctive SAM desorption mechanisms: photoinduced and electrically triggered. The former, occurs concomitantly to hydrogel photocrosslinking with high efficiency eliminating the need for electrical connections and equipment. The latter better maintains cell morphology, preserves monolayer features, and higher cell transfer efficiency over time. In 3D, the combination of SAM-based cell transfer and hydrogel photocrosslinking enables a rapid single-step engineering of micrometric tubular constructs lined with an endothelial cell monolayer. The proposed approach can be used to design more challenging 3D vascular structures, such as double-layer constructs, representing therefore a potentially useful microengineering platform to mimic *in vivo* microvascular organization.

Author contribution

NS, MM, JF and AK designed the study with the contribution of YY; NS and MZ performed the experiments; TO and TK gold coated glass substrates and fabricated culture chambers, NS and MZ analyzed the data; NS wrote the paper; MZ, YY, MM, JF and AK revised the paper. All the authors discussed the results and commented on the paper.

Acknowledgment

This research has been supported by the NIH (HL092836,AK; EB008392, AK; DE019024, AK; HL099073, AK; AR057837, YY; DE021468, YY), NSF and MEXT (Grant-in-Aid for Young Scientists (A), 20686056, Japan, JF). NS acknowledges support provided by the Fondazione Fratelli Agostino and Enrico Rocca through the Progetto Rocca Post Doctoral Fellowship. JF acknowledges support provided by JSPS through Excellent Young Researchers Overseas Visit Program.

References

[1] Lovett M, Lee K, Edwards A, Kaplan DL. Vascularization strategies for tissue engineering. Tissue Eng Part B Rev 2009;15:353–70.
[2] Ko HC, Milthorpe BK, McFarland CD. Engineering thick tissues–the vascularisation problem. Eur Cell Mater 2007;14:1–18. discussion-9.
[3] McGuigan AP, Sefton MV. Vascularized organoid engineered by modular assembly enables blood perfusion. Proc Natl Acad Sci U S A 2006;103:11461–6.
[4] Wong KH, Truslow JG, Tien J. The role of cyclic AMP in normalizing the function of engineered human blood microvessels in microfluidic collagen gels. Biomaterials 2010;31:4706–14.
[5] Villalona GA, Udelsman B, Duncan DR, McGillicuddy E, Sawh-Martinez RF, Hibino N, et al. Cell-seeding techniques in vascular tissue engineering. Tissue Eng Part B Rev 2010;16:341–50.
[6] Norotte C, Marga FS, Niklason LE, Forgacs G. Scaffold-free vascular tissue engineering using bioprinting. Biomaterials 2009;30:5910–7.
[7] Seto Y, Inaba R, Okuyama T, Sassa F, Suzuki H, Fukuda J. Engineering of capillary-like structures in tissue constructs by electrochemical detachment of cells. Biomaterials 2010;31:2209–15.
[8] Fukuda J, Kameoka K, Suzuki H. Spatio-temporal detachment of single cells using microarrayed transparent electrodes. Biomaterials, in press.
[9] Inaba R, Khademhosseini A, Suzuki H, Fukuda J. Electrochemical desorption of self-assembled monolayers for engineering cellular tissues. Biomaterials 2009;30:3573–9.
[10] Hannachi IE, Yamato M, Okano T. Cell sheet technology and cell patterning for biofabrication. Biofabrication 2009;1:022002.
[11] Khademhosseini A, Langer R, Borenstein J, Vacanti JP. Microscale technologies for tissue engineering and biology. Proc Natl Acad Sci U S A 2006;103:2480–7.
[12] Kachouie NN, Du Y, Bae H, Khabiry M, Ahari AF, Zamanian B, et al. Directed assembly of cell-laden hydrogels for engineering functional tissues. Organogenesis 2010;6:234–44.
[13] Ling Y, Rubin J, Deng Y, Huang C, Demirci U, Karp JM, et al. A cell-laden microfluidic hydrogel. Lab Chip 2007;7:756–62.
[14] Nichol JW, Koshy ST, Bae H, Hwang CM, Yamanlar S, Khademhosseini A. Cell-laden microengineered gelatin methacrylate hydrogels. Biomaterials 2010;31:5536–44.
[15] Van Den Bulcke AI, Bogdanov B, De Rooze N, Schacht EH, Cornelissen M, Berghmans H. Structural and rheological properties of methacrylamide modified gelatin hydrogels. Biomacromolecules 2000;1:31–8.
[16] Benton JA, DeForest CA, Vivekanandan V, Anseth KS. Photocrosslinking of gelatin macromers to synthesize porous hydrogels that promote valvular interstitial cell function. Tissue Eng Part A 2009;15:3221–30.
[17] Chen S, Cao Z, Jiang S. Ultra-low fouling peptide surfaces derived from natural amino acids. Biomaterials 2009;30:5892–6.
[18] Vacek K, Geimer J, Beckert D, Mehnert R. Radical generation from photoinitiator (IC 2959) decomposition and radical addition to acrylate. A laser photolysis Fourier transform electron paramagnetic resonance study. J Chem Soc Perkin Trans 1999;2:2469–71.
[19] Hennink WE, Van Nostrum CF. Novel crosslinking methods to design hydrogels. Adv Drug Deliv Rev 2002;54:13–36.
[20] Nguyen KT, West JL. Photopolymerizable hydrogels for tissue engineering applications. Biomaterials 2002;23:4307–14.
[21] Huang J, Hemminger JC. Photooxidation of thiols in self-assembled monolayers on gold. J Am Chem Soc 1993;115:3342–3.
[22] Love JC, Estroff LA, Kriebel JK, Nuzzo RG, Whitesides GM. Self-assembled monolayers of thiolates on metals as a form of nanotechnology. Chem Rev 2005;105:1103–69.
[23] Tarlov MJ, Burgess DRF, Gillen G. UV photopatterning of alkanethiolate monolayers self-assembled on gold and silver. J Am Chem Soc 1993;115:5305–6.
[24] Brewer NJ, Janusz S, Critchley K, Evans SD, Leggett GJ. Photooxidation of self-assembled monolayers by exposure to light of wavelength 254 nm: a static SIMS study. J Phys Chem B 2005;109:11247–56.
[25] Brewer NJ, Rawsterne RE, Kothari S, Leggett GJ. Oxidation of self-assembled monolayers by UV light with a wavelength of 254 nm. J Am Chem Soc 2001;123:4089–90.
[26] Norrod KL, Rowlen KL. Ozone-Induced oxidation of self-assembled decanethiol: contributing mechanism for "Photooxidation"? J Am Chem Soc 1998;120:2656–7.
[27] Wildt B, Wirtz D, Searson PC. Programmed subcellular release for studying the dynamics of cell detachment. Nat Methods 2009;6:211–3.
[28] Okano T, Yamada N, Okuhara M, Sakai H, Sakurai Y. Mechanism of cell detachment from temperature-modulated, hydrophilic-hydrophobic polymer surfaces. Biomaterials 1995;16:297–303.
[29] Ernst O, Lieske A, Jager M, Lankenau A, Duschl C. Control of cell detachment in a microfluidic device using a thermo-responsive copolymer on a gold substrate. Lab Chip 2007;7:1322–9.
[30] Kumashiro Y, Yamato M, Okano T. Cell attachment-detachment control on temperature-responsive thin surfaces for novel tissue engineering. Ann Biomed Eng 2010;38:1977–88.
[31] Weder G, Guillaume-Gentil O, Matthey N, Montagne F, Heinzelmann H, Voros J, et al. The quantification of single cell adhesion on functionalized surfaces for cell sheet engineering. Biomaterials 2010;31:6436–43.
[32] Goldstein AS, DiMilla PA. Examination of membrane rupture as a mechanism for mammalian cell detachment from fibronectin-coated biomaterials. J Biomed Mater Res A 2003;67:658–66.
[33] Huang H, Dong CY, Kwon HS, Sutin JD, Kamm RD, So PT. Three-dimensional cellular deformation analysis with a two-photon magnetic manipulator workstation. Biophys J 2002;82:2211–23.
[34] Yang S, Saif T. Micromachined force sensors for the study of cell mechanics. Rev Sci Instrum 2005;76:044301–8.
[35] Reinhart-King CA, Dembo M, Hammer DA. The dynamics and mechanics of endothelial cell spreading. Biophys J 2005;89:676–89.
[36] Ryan PL, Foty RA, Kohn J, Steinberg MS. Tissue spreading on implantable substrates is a competitive outcome of cell-cell vs. cell-substratum adhesivity. Proc Natl Acad Sci U S A 2001;98:4323–7.

[37] Okochi N, Okazaki T, Hattori H. Encouraging effect of cadherin-mediated cell-cell junctions on transfer printing of micropatterned vascular endothelial cells. Langmuir 2009;25:6947–53.
[38] Flynn NT, Tran TNT, Cima MJ, Langer R. Long-Term stability of self-assembled monolayers in biological media. Langmuir 2003;19:10909–15.
[39] Dejana E, Tournier-Lasserve E, Weinstein BM. The control of vascular integrity by endothelial cell junctions: molecular basis and pathological implications. Dev Cell 2009;16:209–21.
[40] Johnstone S, Isakson B, Locke D. Biological and biophysical properties of vascular connexin channels. Int Rev Cell Mol Biol 2009;278:69–118.
[41] Provost N, Moreau M, Leturque A, Nizard C. Ultraviolet A radiation transiently disrupts gap junctional communication in human keratinocytes. Am J Physiol Cell Physiol 2003;284:C51–9.
[42] Laird DW. Connexin phosphorylation as a regulatory event linked to gap junction internalization and degradation. Biochim Biophys Acta 2005;1711:172–82.
[43] Kawashima T, Yokoi T, Kaji H, Nishizawa M. Transfer of two-dimensional patterns of human umbilical vein endothelial cells into fibrin gels to facilitate vessel formation. Chem Commun (Camb) 2010; 46:2070–2.
[44] Kobayashi A, Miyake H, Hattori H, Kuwana R, Hiruma Y, Nakahama K, et al. In vitro formation of capillary networks using optical lithographic techniques. Biochem Biophys Res Commun 2007;358:692–7.
[45] Chrobak KM, Potter DR, Tien J. Formation of perfused, functional microvascular tubes in vitro. Microvasc Res 2006;71:185–96.
[46] Price GM, Wong KH, Truslow JG, Leung AD, Acharya C, Tien J. Effect of mechanical factors on the function of engineered human blood microvessels in microfluidic collagen gels. Biomaterials 2010;31:6182–9.
[47] Chiu JJ, Chien S. Effects of disturbed flow on vascular endothelium: pathophysiological basis and clinical perspectives. Physiol Rev 2011;91: 327–87.

Biomaterials 32 (2011) 6663–6669

Contents lists available at ScienceDirect

Biomaterials

journal homepage: www.elsevier.com/locate/biomaterials

Spatio-temporal detachment of single cells using microarrayed transparent electrodes

Junji Fukuda*, Yoshiaki Kameoka, Hiroaki Suzuki

Graduate School of Pure and Applied Sciences, University of Tsukuba, 1-1-1 Tennodai, Tsukuba, Ibaraki 305-8573, Japan

ARTICLE INFO

Article history:
Received 12 May 2011
Accepted 24 May 2011
Available online 12 June 2011

Keywords:
Indium tin oxide
Electrochemistry
Gold-thiolate bond
Self-assembled monolayer
Cell detachment
Tissue engineering

ABSTRACT

This paper describes a dynamic cell manipulation approach by which cells can be selectively detached from transparent indium tin oxide (ITO) electrodes via electrochemical desorption of a self-assembled monolayer (SAM) of alkanethiol. Changes in the surface properties of ITO following modification and electrical desorption of the SAM were characterized. By using these reactions on ITO, cells were readily attached and then detached from ITO electrodes in a very rapid manner, with greater than 90% of the cells being detached within 5 min. Furthermore, we fabricated micropatterns of ITO electrodes using photolithography. Cells on the micropatterned ITO electrodes could be detached with single-cell resolution. This approach could potentially lead to on-demand harvesting or elimination of one population from others under microscopy, for a wide range of purposes.

1. Introduction

Development of strategies to design the interface between substrates and cells remains an important challenge in materials science [1]. "Smart" biomaterials that exhibit dynamic changes in interfacial properties, including adherence of cells, are important in a variety of fields, ranging from fundamental cell biology to tissue engineering applications [2–4]. External stimuli such as electrical, thermal, optical, and magnetic fields have typically been used to trigger cell detachment [5,6]. For example, by using a culture surface modified with a thermo-responsive polymer, cells can be detached by reducing the temperature from 37 °C to 20 °C. With this approach, corneal and epithelial cell sheets have been employed for the clinical treatment of corneal disorders and esophageal ulceration following endoscopic surgery, respectively [7,8]. A magnetic field has also been used to attract magnetically labeled cells on a non-adherent surface and subsequently harvest them as a cell sheet by removal of the magnetic force [9].

These dynamic cell detachment technologies that operate via external stimuli are often characterized by spatial resolution, temporal resolution, and reversibility. Thermal and magnetic approaches typically possess high temporal resolution and reversibility. However, because it is difficult to produce a large difference in thermal and magnetic fields in a limited space, these approaches may not be applicable to selective detachment of cells with single-cell resolution. The electrical and optical approaches may possess high spatial and temporal resolutions because localized photo-exposure and fabrication of microelectrode arrays can be achieved with submicron resolution. Electrical approaches for the detachment of cells involve the use of electrically responsive molecules or reactions on the surface of an electrode. For example, two electroactive groups, quinone ester and *O*-silyl hydroquinone, were used to release cell adhesive ligands in response to application of either reductive or oxidative potential, resulting in the selective detachment of adherent cells [10]. Polyelectrolyte layers were also used to electrically detach cells from an electrode [11,12]. In this approach, electrolysis of water induces local pH change and subsequent dissolution of the polyelectrolyte layer, resulting in the detachment of cell sheets. Additionally, hydrogel layers were used to detach cells by electrical disruption of the coupling layers [13]. These approaches can achieve selective detachment of cells from a pattern with a resolution of a few hundred micrometers, but higher spatial resolutions for more precise uses such as the detachment of a single cell have not yet been reported.

Our group has also reported on electrochemical approaches by which cells attached to a gold electrode via alkanethiol self-assemble monolayers (SAMs) can be detached via reductive desorption of the SAM by applying a negative electrical potential [14]. Using this approach, cells were noninvasively detached within 5 min. Because this approach involves no complex chemistry and enables very rapid cell detachment, it will be useful for various applications [14,15]. We considered applying this approach for the

* Corresponding author. Tel.: +81 29 853 4995; fax: +81 29 853 4490.
E-mail address: fukuda@ims.tsukuba.ac.jp (J. Fukuda).

0142-9612/$ – see front matter © 2011 Elsevier Ltd. All rights reserved.
doi:10.1016/j.biomaterials.2011.05.068

spatially selective detachment of cells by fabricating microarrays of gold electrodes and applying a potential to particular microelectrodes. This strategy, however, has a serious practical limitation. Specifically, because there is a large difference in light permeability between glass and gold-coated regions, halation makes it difficult to observe cells on the gold electrodes (Supplemental Fig. 1). Therefore, in the present study, we examined the applicability of transparent ITO electrodes for the detachment of cells along with reductive desorption of the SAM. Furthermore, we investigated whether spatially selective detachment of cells could be conducted while leaving the neighboring cells attached through the use of micropatterned ITO electrodes.

2. Materials and methods

2.1. Materials and reagents

The reagents used for cell culture and tests were purchased from the following commercial sources: Dulbecco's modified Eagle medium (DMEM) and fetal bovine serum (FBS) from Invitrogen, USA; endothelial basal medium-2 (EBM-2, CC-3156) and SingleQuots growth supplements (CC-3162) from Cambrex Bio Science, USA; fluorescent diacetate (FDA) and ethidium bromide (EB) from Wako Pure Chemicals Industries, Japan; Rhodamine phalloidin from Cytoskeleton, Inc., USA; and 4′,6-diamidino-2-phenylindole (DAPI) from Sigma, USA.

Materials used to fabricate the culture substrates were obtained from the following commercial sources: ITO substrate (thickness, 150 nm; resistance, 15 Ω/cm) from Sanyo Vacuum Industries, Japan; 10-carboxy-1-decanethiol from Dojindo Laboratories, Japan; GRGDS peptide from the Peptide Institute, Japan; precursor solution of polyimide (Semicofine SP-341) from Toray, Japan; positive photoresist (Shipley 1818) and MF-319 solution from Rohm and Haas, USA; and liquid prepolymers of poly(dimethylsiloxane) (PDMS, KE-1300T) from ShinEtsu Chemical, Japan. All other chemicals were purchased from Sigma, USA, unless otherwise noted.

2.2. Adsorption and desorption of SAM on ITO

A circular active area (0.4 cm^2) was delineated on an ITO electrode with a photocrosslinkable polyimide insulating layer using a corresponding photomask. The electrode was then cleaned with piranha solution (H_2SO_4:H_2O_2, 3:1) and 1.0% sodium dodecyl sulfate. The electrode surface was covered with a SAM by immersing it in 1 mM 10-carboxy-1-decanethiol in ethanol for 30 min at room temperature. Subsequently, the electrode was rinsed with ethanol and double distilled water. The ITO electrode, a Ag/AgCl reference electrode (#2080 A; Horiba, Japan), and a Pt auxiliary electrode were connected to a potentiostat (Autolab, PGSTAT12, Eco Chemie, The Netherlands). Cyclic voltammograms pertaining to desorption of the SAM were obtained with the three-electrode configuration in a 0.5 M KOH solution that was deoxygenated by bubbling nitrogen gas for 20 min prior to use. In this study, all potential values refer to those measured with respect to the Ag/AgCl electrode.

X-ray photo spectroscopy (XPS) spectra were obtained using a JPS-9010TR photoelectron spectrometer with a monochromatic AL Kα X-ray source (JEOL, Japan). Narrow scans were conducted to obtain the S 2p peak of samples of the bare ITO electrode, ITO electrode modified with the SAM, and ITO electrode after desorption of the SAM by application of −1.0 V for 5 min.

Changes in surface topography following modification of ITO with the SAM were determined by atomic force microscopy (AFM) (5500 AFM, Agilent Technologies Inc., CA, USA) using the acoustic AC mode with a single crystal Si tip, a resonant frequency of 290.3 kHz and a scan speed of 1 μm/s. All images were obtained under atmospheric pressure at room temperature. Images were analyzed using the Pico Image Basic Software (Agilent Technologies Inc.).

2.3. Preparation of cells

Swiss 3T3 murine fibroblasts (RCB1642) were purchased from the Riken Cell Bank, Japan, and maintained in DMEM supplemented with 10% FBS. The medium was changed every other day. Human umbilical vein endothelial cells (HUVECs, CC-2517A) were purchased from Cambrex Bio Science, USA, and maintained in EBM-2 supplemented with SingleQuots growth supplements. The medium was changed every other day. Each passage was conducted in a solution of 0.25% trypsin and 0.02% ethylenediamine tetraacetic acid (EDTA) after 3–4 d for fibroblasts and 2–3 d for HUVECs. Both cells were resuspended in fresh medium and diluted 1:3. HUVECs from passages 3 through 8 were used for the experiments.

2.4. Modification of ITO electrode for cell culture

To promote adhesion of the cells, the carboxyl terminals of the alkanethiol SAM were coupled to a cell adhesion peptide, GRGDS, through carbodiimide-mediated cross-linking as previously described (Fig. 1A) [14]. Growth of cells on the modified electrode was investigated using fibroblasts. Briefly, fibroblasts (1.0×10^5 cells/ml) in 2 mL of culture medium were seeded on a conventional culture dish, bare ITO electrode, and ITO electrode modified with the alkanethiol SAM and RGD. The cells were cultured for four days and the number was measured every day. The cell number was counted based on the number of nuclei using the crystal violet staining method [16].

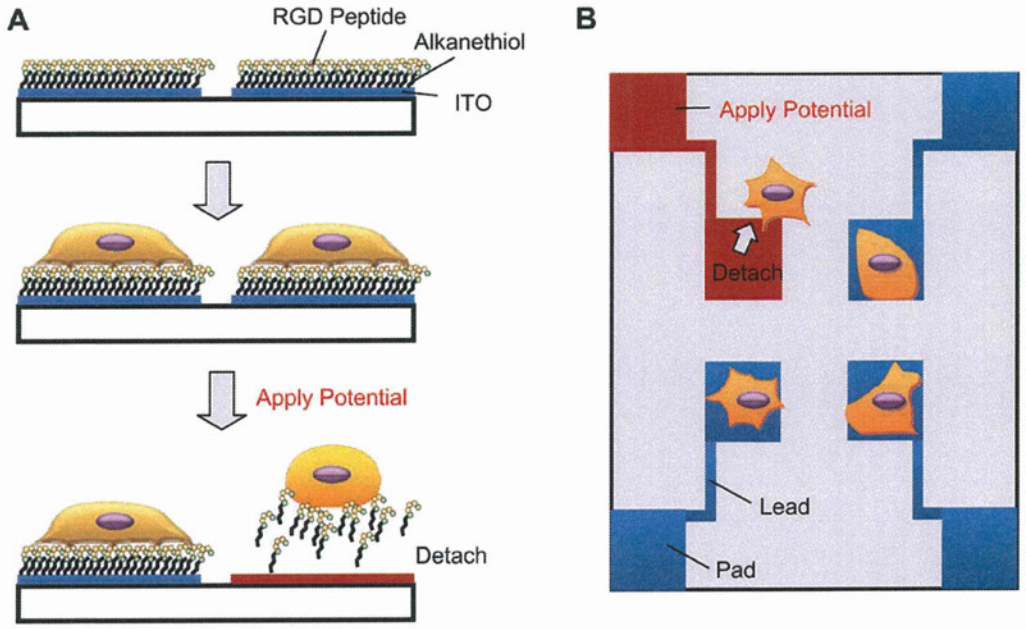

Fig. 1. Detachment of cells in a spatially and temporally controlled manner. (A) Cross-sectional view of micropatterned ITO electrodes. The electrodes were modified with an alkanethiol SAM and RGD peptide. A cell on a specific electrode was detached by applying a negative potential. (B) Top view indicating microelectrodes, electrode leads and pads for the connections to a potentiostat. The schematic is not equivalent to the real dimensions and the cells and microelectrodes were drawn enlarged for clarity of illustration. (For interpretation of the references to colour in this figure legend, the reader is referred to the web version of this article.)

2.5. Electrochemical detachment of cells

Fibroblasts (1.0×10^5 cells/ml) in 2 mL of culture medium were seeded on the modified electrode, after which they were cultured for 12 h at 37 °C in 5% CO_2 in a humidified incubator. The electrode was then washed with PBS three times and connected to a potentiostat (HA-151; Hokuto-Denko, Japan) in PBS. After applying a potential of −1.0 V, the electrode was washed gently with PBS using a pipette, and the cells that remained on the substrate were counted by taking phase-contrast micrographs. For comparison, the same experiments were conducted under conditions in which the cells were attached directly to a bare ITO electrode or no potential was applied.

2.6. Change in cell morphology during electrochemical detachment

Cellular morphology before and after the detachment was investigated using a confocal microscope. Fibroblasts were cultured for 24 h on the modified ITO electrode. Cells before and after the potential application were fixed with 3.7% formaldehyde in PBS for 10 min, after which they were permeabilized with 0.2% Triton X-100 for 5 min. The cells were then incubated with a mixed solution of rhodamine phalloidin and DAPI for 20 min, after which they were rinsed with PBS for 1 min. Images were taken using a confocal microscope (FV1000-D, Olympus, Japan) with a laser diode as the excitation light source for rhodamine-phalloidin and DAPI.

2.7. Micropatterning of ITO electrode and spatially selective detachment of cells

Micropatterns of ITO electrodes were fabricated using photolithography [17]. Briefly, an approximately 100-nm-thick gold layer was initially sputter-coated on an ITO layer by a RF magnetron sputtering (MSP 30T; Vacuum Device, Japan). Next, a positive photoresist was spin-coated onto the gold layer and exposed to UV light through a photomask using a mask aligner (MA-10; MIKASA, Japan). The photoresist patterns were then developed in MF-319 solution for 5 min, after which the samples were washed with DI water and dried. The gold layer was then etched by immersion in an aqueous solution containing 0.1 g/ml potassium iodide and 25 mg/ml iodine for 5 min. Subsequently, the ITO layer was etched by immersion in an aqueous solution containing 28% (v/v) nitric acid and 31% (v/v) hydrochloric acid for 8 min. The remaining photoresist and gold layer were completely removed using the acetone and etching solution. The micropatterned ITO electrode was then modified with the alkanethiol SAM and RGD peptide using the same procedures described earlier. Fibroblasts were seeded onto the electrode and cultured for 24 h. The cells on the electrode micropattern were then sequentially detached by applying −1.0 V for 5 min.

3. Results and discussion

3.1. Electrical desorption of SAMs

Alkanethiol SAMs have been extensively examined on gold to investigate the effects of surface nature, including surface wettability and charges, on protein adsorption and cell adhesion [18,19]. Despite a large body of literature regarding alkanethiol SAMs on gold, studies regarding ITO are relatively rare [20,21]. In this decade, the use of ITO has promoted the revolution in electronics through their use in items such as touch panels and solar batteries. The preferable features of transparent ITO may also be beneficial for cell-based systems.

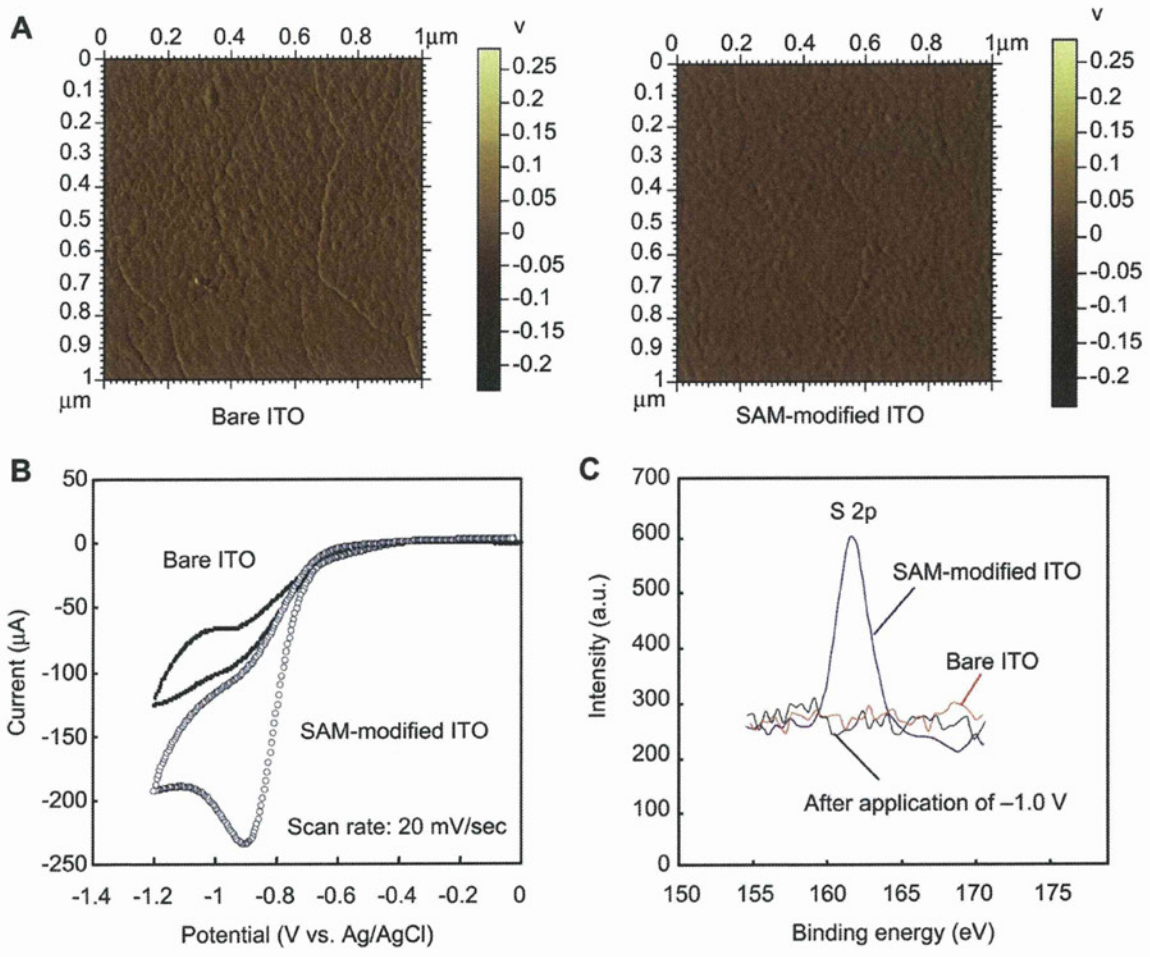

Fig. 2. Characterizations of ITO modified with the SAM. (A) AFM images of bare ITO and ITO after adsorption of the oligopeptide. The scanning areas are 1 × 1 µm. (B) Cyclic voltammogram observed during reductive desorption of the SAM. Cyclic voltammograms were recorded at a scanning rate of 20 mV/s with respect to a Ag/AgCl reference electrode. The working electrode area is 0.4 cm^2 (C) XPS spectra observed for samples of bare ITO, ITO modified with the alkanethiol SAM, and ITO after the application of −1.0 V for 5 min. (For interpretation of the references to colour in this figure legend, the reader is referred to the web version of this article.)

The ITO surface structure largely depends on the fabrication condition, which influences the formation of a well-packed and ordered SAM and reproducibility of experiments [20]. The surface topography of ITO was examined using AFM prior to use. The ITO surfaces presented crystalline grains (Fig. 2A). ITO with a maximal height difference less than 25 nm was used for this study. It should be noted that on the basis of AFM analysis the surface topography was not significantly altered by the treatment processes for the modification with 10-carboxy-1-decanethiol in ethanol (Fig. 2A) or the electrical desorption of the SAM (data not shown). The potential required for desorption of the SAM from ITO was estimated using cyclic voltammetry. As shown in Fig. 2B, a peak potential appeared at approximately −0.9 V. Although the interaction on an atomic level between ITO and thiol (unlike gold and thiol) has not yet been clarified, this value is very close to that observed on a gold surface in our previous study [14,15]. XPS measurements were conducted to investigate changes in chemical bonding in the formation and desorption of the SAM on ITO [21]. Fig. 2C shows the high-resolution XPS spectra for bare ITO, ITO modified with the SAM, and ITO electrode after desorption of the SAM by application of −1.0 V for 5 min. A clear peak corresponding to the S 2p orbital at 162 eV was observed for the SAM-modified ITO, whereas no peak was observed for the bare ITO or the ITO modified with the SAM and treated with an electrical potential. These electrochemical and XPS results indicate that the alkanethiol spontaneously adsorbed onto the ITO electrode and was then reductively desorbed by application of the potential. Based on these results, we decided to use −1.0 V for desorption of the SAM and detachment of cells in the following experiments.

3.2. Change in cell morphology during electrochemical detachment

The ITO electrode modified with the SAM and RGD peptide was used to investigate cell proliferation and the electrochemical detachment of cells. Fibroblasts were readily attached and spread out on the modified ITO electrode (Fig. 3A). The number of cells was then counted every day for four days. The proliferation of fibroblasts on the electrode (doubling time, 20 ± 3.5 h) was slightly slower than that on a typical culture dish (16 ± 1.5 h) and that reported in the literature (16.6 h), but these differences were not significant [22]. At 24 h of culture, fibroblasts adhering to the electrode were detached by applying a potential of −1.0 V Fig. 3B shows the change in cell morphology at 40 s intervals during the detachment. The cells were gradually detached from their edges

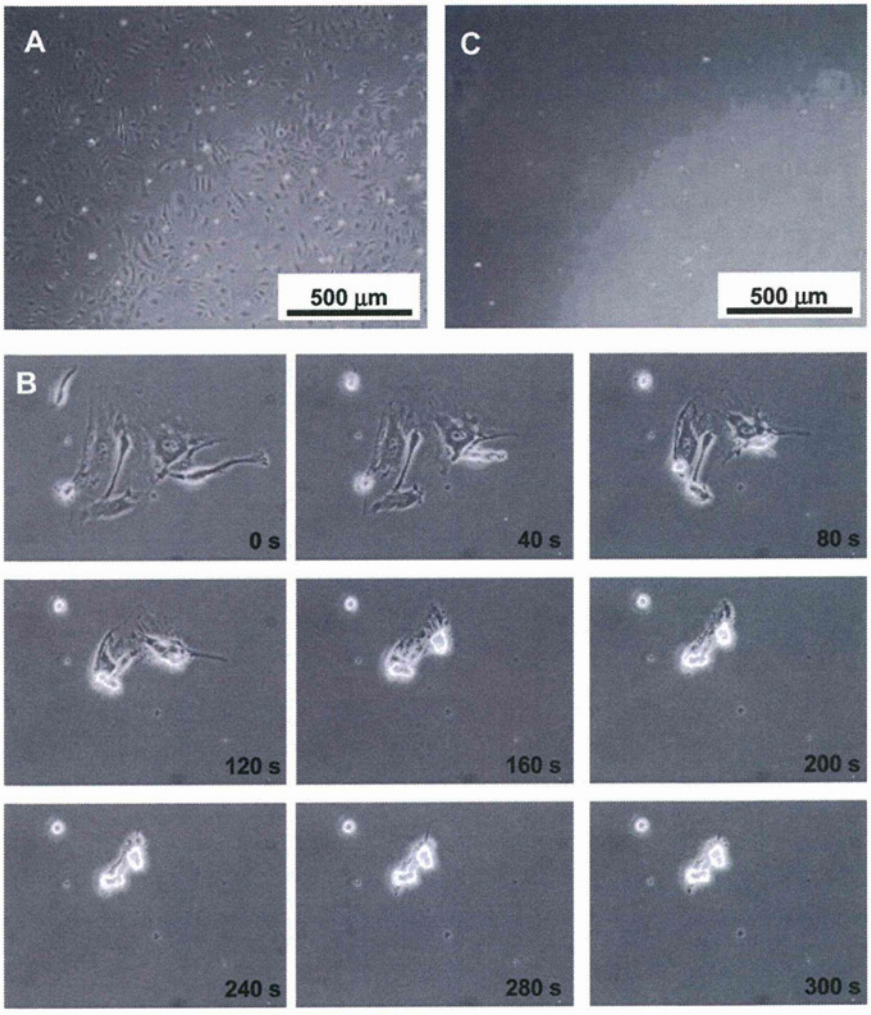

Fig. 3. Detachment of fibroblasts from the ITO electrode. (A) Cells attached to the ITO electrode modified with the SAM and RGD peptide and cultured for 24 h. (B) Changes in cell morphology during the application of −1.0 V were monitored at 40 s intervals. (C) After application of potential for 5 min the cells were identified for detachment by gentle pipetting.

and appeared bright after application of the potential, after which they were identified for detachment by gentle pipetting (Fig. 3C). Changes in the cell shape were also observed and characterized by confocal microscopy after staining of the F-actin and nuclei (Fig. 4). The top and side views show that the extended cells had a bulge at the nucleus and stress fibers (Fig. 4A and B). Image analysis of these cells revealed that the approximate height and width before application of the potential were 7.9 μm and 74 μm, respectively (Fig. 4E and F). These cells were rounded after applying the potential (Fig. 4C and D). In this process, the width decreased to approximately 13 μm, whereas the height only increased to about 12 μm (Fig. 4E and F). It should be noted that Fig. 4A and C represent full stacks of confocal images and Fig. 4B and D represent stacks of images from the bottom to the middle of the cell. The dynamic cell attachment/detachment to and from extracellular microenvironments *in vivo* regulates cell growth, differentiation, and apoptosis [23]. The relationships between the formation of focal adhesion complexes at the interface and a wide range of signal transduction and gene expression have typically been examined using the adhesion process of suspended cells [24]. This approach could potentially enable focal adhesion disassembly and subsequent remodeling of the cytoskeleton using the cell detachment process.

3.3. Quantitative analysis of the detachment of cells

To quantitatively analyze the detachment of cells, the number of fibroblasts that remained on the surface following application of the potential was counted at 60 s intervals (Fig. 4G). Cells were attached to the bare ITO well probably due to adhesion proteins in FBS and there was no significant difference in the number of cells initially attached onto the ITO electrode with or without modification with the SAM and RGD ($1.5–2 \times 10^4$ cells/cm^2). When the SAM and an electrical potential of −1.0 V were used, more than 90% of the cells were detached from the surface within 5 min. To the best of our knowledge, this is the most rapid cell detachment approach that has been reported to date. In the control experiments (no SAM or no potential application), the behavior of the cells was clearly different as shown in Fig. 4G. These results suggest that electrical desorption of the SAM is primarily responsible for the detachment of cells. Note that approximately 30% of the cells were detached in the control experiment (conditions of no SAM and −1.0 V). This was likely because some cells attached onto the bare ITO via proteins and were detached together with proteins in response to application of the potential.

3.4. Spatially controlled detachment of cells

To selectively detach cells on demand, a micropattern of ITO electrodes was fabricated via wet etching and the electrodes were then modified with the SAM and RGD peptide. The spacing between the electrodes was 50 μm. As shown in Fig. 5, cells adhering to the ITO microelectrodes were clearly observed upon phase-contrast microscopy. Cells adhering onto the microelectrodes were electrically detached one by one. A cell on the electrode labeled 1 was detached by application of the potential for 5 min as shown in Fig. 5B. It should be noted that there was no influence on the cells on the neighboring electrodes during this detachment. Similarly, cells on the other electrodes were detached sequentially in numerical order as shown in Fig. 5B–D.

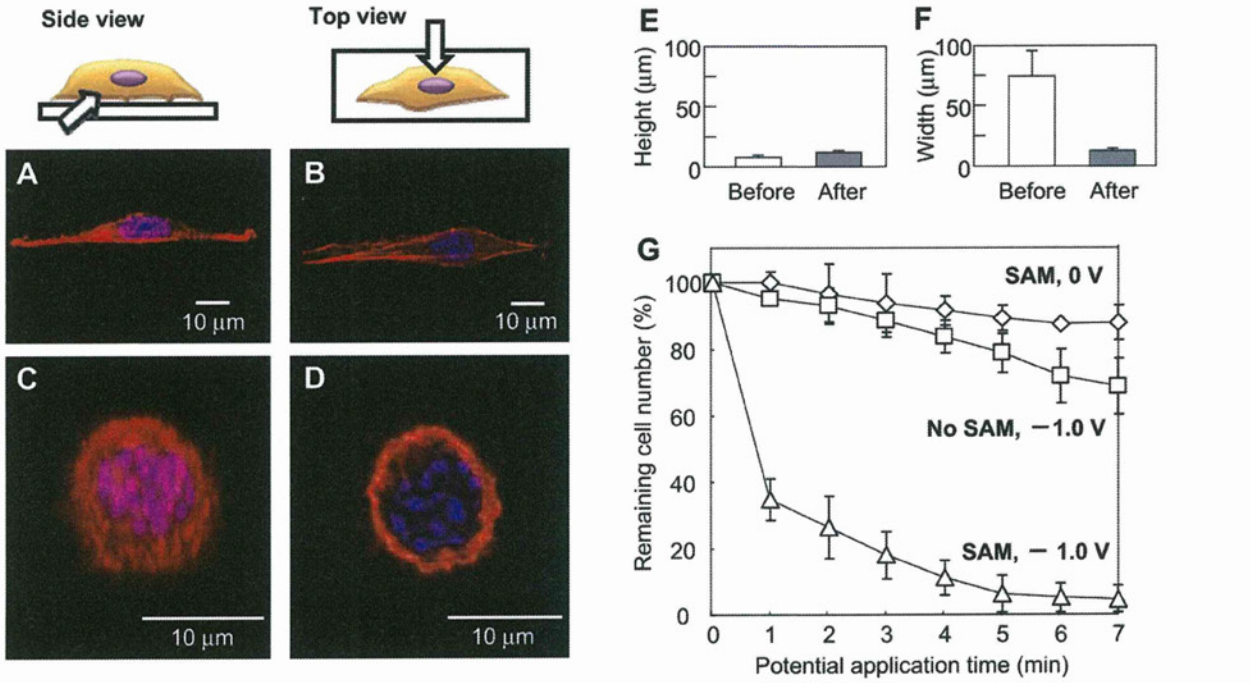

Fig. 4. Changes in cell shape of fibroblasts and quantitative analysis of cell detachment. (A–D) Representative images of a fibroblast before (A and B) and after (C and D) application of potential. Rhodamine-phalloidin was used to stain actin fibers red and DAPI was used to stain nuclei blue. Side views (A and C) indicate images constructed by stacking optically sectioned images of an entire cell from edge to edge, and top views (B and D) indicate images constructed by stacking images from the bottom to the middle of the cell. (E, F) Image analysis was conducted to obtain quantitative data regarding the cell height (E) and width (F) before and after the potential application. The values indicate the mean of four independent experiments. Error bars indicate the SD. (G) Changes in the number of fibroblasts remaining on the ITO electrode. More than 90% of the cells were detached from the surface after application of the potential for 5 min along with desorption of the SAM (SAM, −1.0 V). Significantly lower numbers of cells were detached from the surface when the cells were attached directly onto a bare ITO electrode (no SAM, 0 V) or when no potential was applied (SAM, 0 V). The values indicate the mean of nine independent experiments. Error bars indicate the SD. (For interpretation of the references to colour in this figure legend, the reader is referred to the web version of this article.)

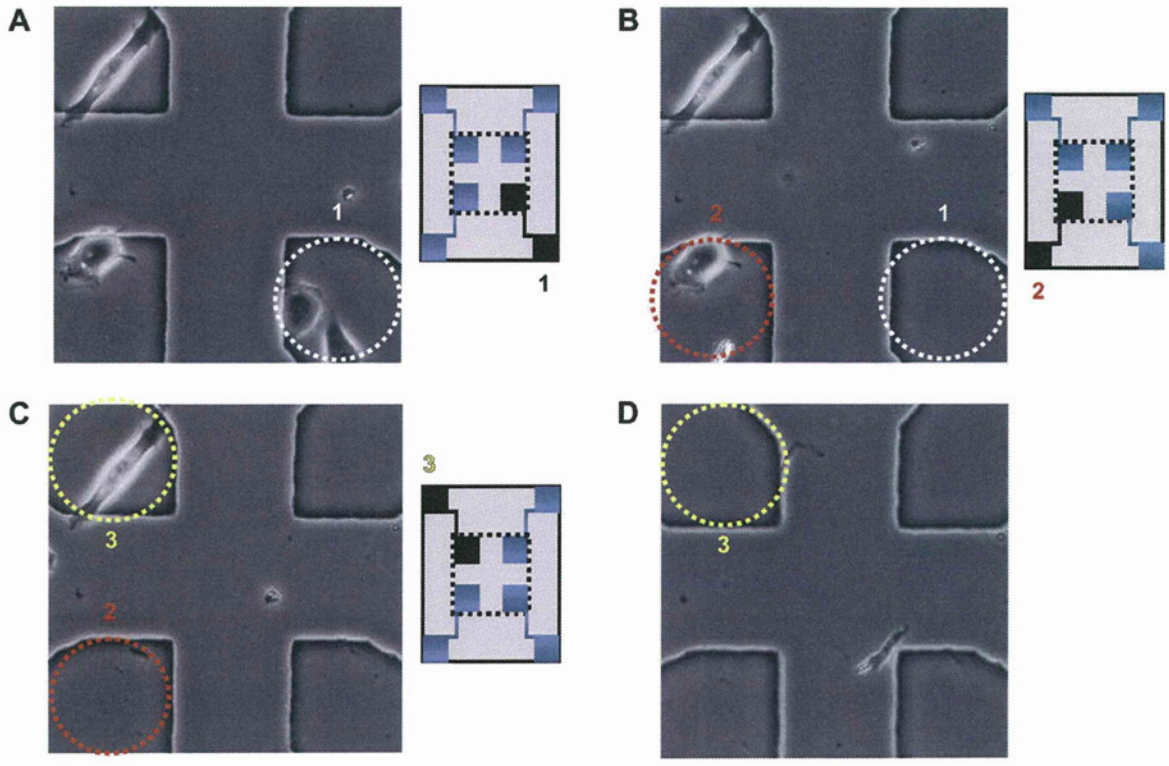

Fig. 5. Selective detachment of cells using a micropatterned ITO electrode. HUVECs attached onto the microelectrodes were sequentially detached by applying the potential to the electrodes in the numerical order of labeled digits. The spacing between the electrodes was 50 μm. (A) The circle labeled 1 indicates the initially activated electrode. (B) Cells on the electrode labeled 1 were detached. The circle labeled 2 indicates the subsequently activated electrode. (C) The cells on the electrode labeled 2 were detached. The circle labeled 3 indicates the activated electrode. (D) The cell on the electrode labeled 3 was detached. (For interpretation of the references to colour in this figure legend, the reader is referred to the web version of this article.)

The selective cell detachment could potentially be useful in fundamental cell biology as well as cell processing for regenerative medicine. In the field of regenerative medicine, considerable efforts have been focused on inducing differentiation of iPS cells or ES cells to a specific cell type [25]. However, the multipotency of stem cells makes this process difficult. Because our technology has enabled access to cells being observed under a microscope, it may be possible to alleviate this issue by eliminating undesired cell populations from culture based on estimation of cell fate from their shapes on a culture surface. In the present study, we only fabricated four microelectrodes as proof of concept. However, in the semiconductor industry, the precision of microfabrication technologies has already reached the nano meter scale. Our next goal is to fabricate ITO microelectrodes with dimensions smaller than those of a cell.

4. Conclusion

We revealed that an alkanethiol molecule spontaneously adsorbs onto ITO, and can then be reductively desorbed by the application of potential. Using this dynamic reaction, cells were detached in a reliable and rapid manner, with more than 90% of adherent cells being electrically detached by application of potential for 5 min. Furthermore, owing to the transparency of ITO, cells on the microarray of ITO electrodes could be clearly observed using conventional phase-contrast microscopy and were selectively detached on-demand. Although this is a rapid cell detachment approach, considering that desorption of the SAM was completed within 1 min during cyclic voltammetry analysis, there may be room for acceleration of the detachment of cells. This study did not focus on the crystalline architecture of ITO or orientation of SAM, which may be largely responsible for the electrical cell detachment. It still remains to be seen whether atomically flat ITO epitaxial film can hasten the processes described herein [26]. This electrical cell detachment could be a fundamental tool in diverse research fields, ranging from fundamental cell biology to tissue engineering applications.

Acknowledgments

This study was supported by the Ministry of Education, Culture, Sports, Science and Technology (Grant-in-Aid for Young Scientists (A), 20686056), the Ministry of Health, Labor and Welfare (H20-Saisei-wakate-010), and NEDO (Industrial Technology Research Grant Program, 06A06014a).

Appendix. Supplementary material

Supplementary data associated with this article can be found, in the online version, at doi: 10.1016/j.biomaterials.2011.05.068.

References

[1] Langer R, Tirrell DA. Designing materials for biology and medicine. Nature 2004;428(6982):487–92.
[2] Lahann J, Mitragotri S, Tran TN, Kaido H, Sundaram J, Choi IS, et al. A reversibly switching surface. Science 2003;299(5605):371–4.
[3] Matsuda N, Shimizu T, Yamato M, Okano T. Tissue engineering based on cell sheet technology. Adv Mater 2007;19(20):3089–99.
[4] Fukuda J, Khademhosseini A, Yeh J, Eng G, Cheng JJ, Farokhzad OC, et al. Micropatterned cell co-cultures using layer-by-layer deposition of extracellular matrix components. Biomaterials 2006;27(8):1479–86.

[5] Cole MA, Voelcker NH, Thissen H, Griesser HJ. Stimuli-responsive interfaces and systems for the control of protein-surface and cell-surface interactions. Biomaterials 2009;30(9):1827–50.
[6] Nandivada H, Ross AM, Lahann J. Stimuli-responsive monolayers for biotechnology. Prog Polym Sci 2010;35(1–2):141–54.
[7] Elloumi-Hannachi I, Yamato M, Okano T. Cell sheet engineering: a unique nanotechnology for scaffold-free tissue reconstruction with clinical applications in regenerative medicine. J Intern Med 2010;267(1):54–70.
[8] Nishida K, Yamato M, Hayashida Y, Watanabe K, Yamamoto K, Adachi E, et al. Corneal reconstruction with tissue-engineered cell sheets composed of autologous oral mucosal epithelium. N Engl J Med 2004;351(12):1187–96.
[9] Kamihira M, Akiyama H, Ito A, Kawabe Y. Genetically engineered angiogenic cell sheets using magnetic force-based gene delivery and tissue fabrication techniques. Biomaterials 2010;31(6):1251–9.
[10] Yeo WS, Mrksich M. Electroactive self-assembled monolayers that permit orthogonal control over the adhesion of cells to patterned substrates. Langmuir 2006;22(25):10816–20.
[11] Guillaume-Gentil O, Akiyama Y, Schuler M, Tang C, Textor M, Yamato M, et al. Polyelectrolyte coatings with a potential for electronic control and cell sheet engineering. Adv Mater 2008;20(3):560–5.
[12] Guillaume-Gentil O, Gabi M, Zenobi-Wong M, Voros J. Electrochemically switchable platform for the micro-patterning and release of heterotypic cell sheets. Biomed Microdevices 2011;13(1):221–30.
[13] Kim M, Lee JY, Shah SS, Tae G, Revzin A. On-cue detachment of hydrogels and cells from optically transparent electrodes. Chem Comm 2009;(39):5865–7.
[14] Inaba R, Khademhosseini A, Suzuki H, Fukuda J. Electrochemical desorption of self-assembled monolayers for engineering cellular tissues. Biomaterials 2009;30(21):3573–9.
[15] Seto Y, Inaba R, Okuyama T, Sassa F, Suzuki H, Fukuda J. Engineering of capillary-like structures in tissue constructs by electrochemical detachment of cells. Biomaterials 2010;31(8):2209–15.
[16] Gillies RJ, Didier N, Denton M. Determination of cell number in monolayer-cultures. Anal Biochem 1986;159(1):109–13.
[17] Suzuki M, Yasukawa T, Shiku H, Matsue T. Separation of live and dead microorganisms in a micro-fluidic device by dielectrophoresis. Bunseki Kagaku 2005;54(12):1189–95.
[18] Ulman A. An introduction to ultrathin organic films - from Langmuir-Blodgett to self-assembly. Academic Press; 1991. pp. 279–296.
[19] Sigal GB, Mrksich M, Whitesides GM. Effect of surface wettability on the adsorption of proteins and detergents. J Am Chem Soc 1998;120(14):3464–73.
[20] Cerruti M, Rhodes C, Losego M, Efremenko A, Maria JP, Fischer D, et al. Influence of indium-tin oxide surface structure on the ordering and coverage of carboxylic acid and thiol monolayers. J Phys D Appl Phys 2007;40(14):4212–21.
[21] Yan C, Zharnikov M, Golzhauser A, Grunze M. Preparation and characterization of self-assembled monolayers on indium tin oxide. Langmuir 2000;16(15):6208–15.
[22] Rossow PW, Riddle VG, Pardee AB. Synthesis of labile, serum-dependent protein in early G1 controls animal cell growth. Proc Natl Acad Sci USA 1979;76(9):4446–50.
[23] Huang S, Ingber DE. Shape-dependent control of cell growth, differentiation, and apoptosis: switching between attractors in cell regulatory networks. Exp Cell Res 2000;261(1):91–103.
[24] Dobereiner HG, Dubin-Thaler B, Giannone G, Xenias HS, Sheetz MP. Dynamic phase transitions in cell spreading. Phys Rev Lett 2004;93(10):4.
[25] Snykers S, De Kock J, Rogiers V, Vanhaecke T. In vitro differentiation of embryonic and adult stem cells into hepatocytes: state of the art. Stem Cells 2009;27(3):577–605.
[26] Ohta H, Orita M, Hirano M, Tanji H, Kawazoe H, Hosono H. Highly electrically conductive indium-tin-oxide thin films epitaxially grown on yttria-stabilized zirconia (100) by pulsed-laser deposition. Appl Phys Lett 2000;76(19):2740–2.

JOURNAL OF TISSUE ENGINEERING AND REGENERATIVE MEDICINE
J Tissue Eng Regen Med 2013; 7: 236–243.
Published online 12 December 2011 in Wiley Online Library (wileyonlinelibrary.com) **DOI:** 10.1002/term.519

RESEARCH ARTICLE

Tissue engineering based on electrochemical desorption of an RGD-containing oligopeptide

Naoto Mochizuki[1], Takahiro Kakegawa[1], Tatsuya Osaki[1], Nasser Sadr[2], Nezamoddin N. Kachouie[2,3], Hiroaki Suzuki[1] and Junji Fukuda[1]*

[1]*Graduate School of Pure and Applied Sciences, University of Tsukuba, 1-1-1 Tennoudai, Tsukuba, Ibaraki, 305-8573, Japan*
[2]*Harvard–MIT Division of Health Sciences and Technology, Massachusetts Institute of Technology, Cambridge, MA, USA*
[3]*Department of Medicine, Brigham and Women's Hospital, Harvard Medical School, Cambridge, MA, USA*

Abstract

This paper describes a non-invasive approach for efficient detachment of cells adhered to a gold substrate via a specific oligopeptide. Detachment is effected by an electrical stimulus. The oligopeptide contains cysteine, which spontaneously forms a gold–thiolate bond on a gold surface. This chemical adsorption reaches > 95% equilibrium within 10 min after immersion of a gold-coated substrate in a solution containing the peptide. The peptide is reversibly desorbed from the surface within 5 min of application of a negative electrical potential. By taking advantage of this simple adsorption and desorption mechanism, cells can be grown on an oligopeptide-functionalized gold surface and can be efficiently detached as single cells or cell sheets by application of a negative electrical potential. This approach was also applied to the surface of gold-coated microrods. Capillary-like microchannels were formed in collagen gel by transferring endothelial cells to the internal surfaces of the microchannels. During subsequent perfusion culture, the enveloped endothelial cells migrated into the collagen gel and formed luminal structures, which sprouted from the microchannels. This technique has the potential to provide a fundamental tool for the engineering of thick cell sheets as well as vascularized tissues and organs.

Received 21 March 2011; Revised 7 July 2011; Accepted 22 September 2011

Keywords **cell sheet; blood vessel; oligopeptide; electrochemistry; gold–thiolate bond; fibroblast; human umbilical vein endothelial cells; collagen**

1. Introduction

A major approach in tissue engineering is the use of scaffolds composed of biodegradable synthetic polymers or extracellular matrix (Langer and Vacanti, 1993). This approach has proved to be beneficial for the reconstruction of several types of tissues and has been increasingly translated to successful clinical applications (Atala, 2009). However, some issues remain to be addressed, including mismatches between scaffolds and native matrices, spatial and temporal differences between cell growth and scaffold degradation, a lack of proper vasculature and the tissue-like organization of different cell types (Kohane and Langer, 2008; Sung *et al.*, 2004; Khademhosseini *et al.*, 2006). Another promising approach is the use of cell-dense aggregates, such as cell sheets and spheroids (Ohashi *et al.*, 2007; Mironov *et al.*, 2009; Nichol and Khademhosseini, 2009; Fukuda *et al.*, 2006a, 2006b). The manipulation and transplantation of such cell aggregates rely on innovative strategies for non-invasive cleavage of cell-to-culture substrate connections while preserving cell-to-cell connections (Inaba *et al.*, 2009). For example, cell sheets adhered to a thermo-responsive polymer can be detached by controlling the hydrophilicity of the surface with temperature modulation (Ohashi *et al.*, 2007; Okano, 2008). This technique was used to fabricate oral mucosal epithelial cell sheets for reconstruction of corneal tissue in a clinical trial (Nishida *et al.*, 2004). Similarly, microwells consisting of a thermoresponsive hydrogel have been used to generate spheroids that were subsequently released by altering the temperature (Tekin *et al.*, 2010). However, a drawback of these approaches is that relatively long time periods are required to detach cell sheets or spheroids from the substrates (Kwon *et al.*, 2003). Thus, the development of biocompatible and easily applicable approaches for rapid collection of

*Correspondence to: J. Fukuda, Graduate School of Pure and Applied Sciences, University of Tsukuba, 1-1-1 Tennoudai, Tsukuba, Ibaraki 305–8573, Japan.
E-mail: fukuda@ims.tsukuba.ac.jp

cell-dense constructs is desired to assist the process of building *in vivo*-like structures for tissue-engineering applications.

In this paper, we present an electrochemical method for non-invasive detachment of cells from a surface (Figure 1). Cells were cultured on a layer of synthetic oligopeptide adsorbed onto a gold surface. The peptide contained RGD (arginine–glycine–aspartate) in the centre and cysteine residues at both ends. The peptide adsorbed onto the gold surface via a gold–thiolate bond, which mediates cell adhesion to the substrate. The peptide was then reductively desorbed from the gold substrate by the application of a negative electrical potential. This caused the cells to detach from the gold surface in a rapid and reliable manner while maintaining cell–cell connections (Seto *et al.*, 2010; Sadr *et al.*, 2011). In this study, we showed that as a first possible application, this technology can be used to fabricate cell sheets and microcapillary-like structures.

2. Materials and methods

2.1. Materials and reagents

Swiss 3 T3 murine fibroblasts (RCB1642) were purchased from Riken Cell Bank, Japan. Human umbilical vein endothelial cells (HUVECCC-2517A), endothelial basal medium-2 (EBM-2, CC-3156) and SingleQuots growth supplement (CC-3162) were purchased from Cambrex Bio Science, USA. The other reagents used for cell culture and tests included Dulbecco's modified Eagle's medium (DMEM) and fetal bovine serum (FBS; Invitrogen, USA); phorbol-12-myristate-13-acetate (PMA; Sigma-Aldrich, Japan); collagen type I (Cellmatrix Type I-A; Nitta Gelatin, Japan); fluorescent diacetate (FDA) and ethidium bromide (EB; Wako Pure Chemical Industries, Japan); DAPI (Sigma-Aldrich); and rhodamine–phalloidin (Cytoskeleton, USA).

The materials used in the fabrication of culture substrates were as follows: glass wafers (No. 7740; diameter 3 inches; thickness 500 μm; Corning, USA); glass rods (diameter 600 μm; length 3.2 cm; Hirschmann Laborgeräte, Germany); and synthetic oligopeptide (CCRRGDWLC; Sigma-Aldrich). All other chemicals were purchased from Wako Pure Chemical Industries, unless otherwise indicated.

2.2. Modification of gold substrates with the oligopeptide

The oligopeptide CCRRGDWLC contains an RGD domain in the centre and cysteine residues at both ends (Figure 1A). The oligopeptide is designed such that cells adhere onto a gold surface via the oligopeptide and are detached by an electrical stimulus. A gold surface was prepared by sputter-coating a layer of Cr a few nanometers thick and a 40 nm layer of Au on either a glass wafer or a glass rod (diameter 600 μm). The wafer was then cut into 15 × 10 mm pieces. These gold surfaces were modified by immersing them into 0.5 μM aqueous solutions of the oligopeptide overnight at 4 °C. After washes with double-distilled water, the substrates were sterilized with 70% ethanol before cell culture.

2.3. Monitoring of adsorption and electrochemical desorption of the oligopeptide

The adsorption of the peptide onto the gold surface was monitored using a quartz crystal microbalance (QCM, AFFINIX-QN; Initium, Tokyo, Japan). Gold electrodes on

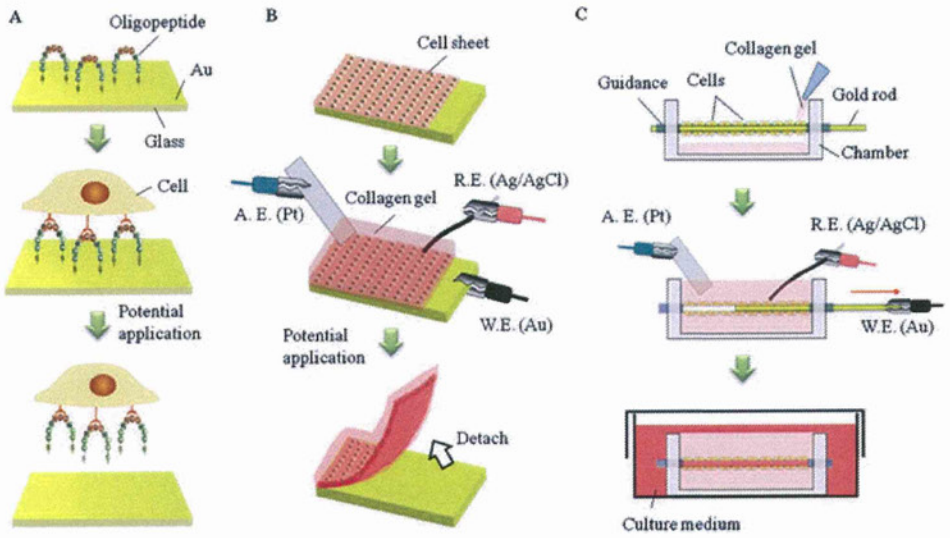

Figure 1. Detachment of cells by application of an electrical potential. (A) Principle of cell detachment: cells adhered to the gold surface via the adsorbed oligopeptide, CCRRGDWLC, were detached during the reductive desorption of the oligopeptide. (B) Cell sheet: cells were grown to form a cell sheet on the gold surface. After addition of a collagen gel to facilitate handling, the cell sheets were detached from the surface by the application of an electrical potential and collected as single entire cell sheets. (C) Capillaries: thin gold rods covered with HUVECs were aligned in a chamber. Upon application of a potential and extraction of the rods from the chamber, the cells were transferred onto the surface of capillaries in collagen gel. Subsequent culture induced migration and sprouting in the gel

the QCM (250 ± 50 nm layer of gold) were cleaned with piranha solution (H_2SO_4:H_2O_2, 3:1) and 1% sodium dodecyl sulphate. The QCM was then set in 8 ml pure water, and 4 μL of a 1 mM aqueous solution of the oligopeptide (final concentration: 0.5 μM) was added with stirring. The amount of adsorbed oligopeptide was determined by the change in resonance frequency according to Sauerbrey's equation.

Cyclic voltammetry was employed to determine the reductive potential for desorption of the oligopeptide adsorbed on the gold surface. Immediately before cyclic voltammetry was performed, an electrolyte solution containing 0.5 M KOH was deoxygenated by bubbling nitrogen gas for 20 min. The oligopeptide-modified gold substrate, a Ag/AgCl reference electrode (No. 2080 A; Horiba, Tokyo, Japan), and a platinum auxiliary electrode were set in the electrolyte solution and connected to an electrochemical measurement system (Autolab; Metrohm Autolab, The Netherlands). A cyclic voltammogram was recorded at the scanning rate of 20 mV/s in the range 0–1.0 V three times. All potential values refer to those measured with respect to a Ag/AgCl electrode.

Changes in surface topography after adsorption and desorption of the oligopeptide were determined by atomic force microscopy (AFM; 5500 AFM, Agilent Technologies, CA, USA) using the acoustic AC mode with a single crystal Si tip with a resonant frequency of 290.3 kHz and a scan speed of 1 μm/s. All images were obtained under atmospheric pressure at room temperature. Images were analysed using commercial DI software; PicoImageBasic (Agilent).

2.4. Preparation of cells

Swiss 3 T3 murine fibroblasts were maintained in DMEM supplemented with 10% FBS. HUVECs were maintained in EBM-2 supplemented with SingleQuots growth supplement. HUVECs from passages 3–8 were used for experiments. The media were changed every other day. Cell passage was conducted with a solution of 0.25% trypsin and 0.02% ethylenediamine tetra-acetic acid (EDTA) after 3–4 days.

2.5. Detachment of single cells

Fibroblasts (0.5×10^5 cells/ml) in 2 ml culture medium were seeded on the flat substrate modified with oligopeptide and were cultured for 2 days at 37 °C in 5% CO_2 in a humidified incubator. The substrates were then washed with PBS three times and connected to a potentiostat (HA-151; Hokuto-Denko, Tokyo, Japan). A Ag/AgCl reference electrode and a platinum auxiliary electrode were also set in the PBS solution and connected to the potentiostat. After application of a potential of −1.0 V for 5 min, the substrates were gently washed with PBS and the attached cells were counted under a microscope. The solution containing the detached cells was transferred into a conventional culture dish to investigate whether the reseeded cells maintained their ability to grow after electrochemical detachment.

Phase-contrast images of the cells on the gold coated surface were obtained using an Olympus inverted microscope (IX-71, Olympus Co., Japan). Shape features (projected area, perimeter) of individual cells were extracted from the phase-contrast images using image analysis software (Photoshop, Adobe Systems, CA, USA). Cell circularity was calculated using the following formula:

$$\text{circularity} = 4\pi(\text{area})/\text{perimeter}^2$$

as previously described (Kazmers *et al.*, 2009). A circularity of 1.0 indicates perfect circular morphology and 0.0 indicates a line.

2.6. Scanning electron microscopy

To observe cells on the glass substrate under a scanning electron microscope (SEM), we washed the culture three times with PBS and fixed with a mixed solution of 2.5% glutaraldehyde and 2% formaldehyde in PBS for 1 h at room temperature. Thereafter, the culture was washed with PBS and fixed with 1% osmium tetroxide in PBS for 1 h at 4 °C. The culture was washed with purified water and dehydrated with a graded ethanol series in the range 30–90% on ice and absolute ethanol substitution three times at room temperature. The solution was further substituted with 100% *t*-butanol, which was frozen at 4 °C and dried by vacuum freeze drying. The cells were observed under an SEM (TM-5000; Hitachi, Japan) operated at 15 kV.

2.7. Detachment of cell sheets

Fibroblasts (1.25×10^5 cells/ml) in 2 ml culture medium were seeded onto the flat substrates. The cells were cultured for 7 days until the cells covered the entire surface of the substrate. The cell sheets were then detached by application of a voltage of −1.0 V for 10 min. Cell viability after the detachment was evaluated using a live/dead fluorometric assay with FDA and EB.

To stain a cross-section of cell sheets with haematoxylin and eosin (H&E), a few drops of type I collagen solution (0.24% w/v) were poured onto the sheet and gelled in a humidified incubator for 30 min at 37 °C to facilitate the subsequent manipulations. Subsequently, by application of a potential of −1.0 V for 10 min and peeling off the gel layer, the cell sheet covered with collagen gel was collected from the culture surface (Figure 1B). The sheet was fixed with 3.7% formaldehyde in PBS, embedded in paraffin and sectioned. H&E staining was performed after the general procedure.

2.8. Fabrication of capillary-like structures

The chamber used for the formation of capillary-like structure (Figure 1C) was fabricated with a poly(methyl

methacrylate) plate by using computer-aided laser machining (Laser PRO C180; GCC, Taiwan). The volume of the chamber was 0.5 ml. The chamber had three pairs of holes of 800 μm diameter at intervals of 500 μm for the guidance of the gold rods.

The gold rods (600 μm in diameter) modified with the oligopeptide were placed in a non-adherent 35 mm dish (Techno Plastic Products, Switzerland) and seeded with HUVECs (3.0×10^5 cells) in 2 ml culture medium. The cells, which adhered to the gold rods, were cultured and grown to reach confluence for 3–4 days.

The gold rods with cells were transferred to the chamber and 0.5 ml of the collagen solution was poured into the chamber and gelled in an incubator at 37 °C. Subsequently, a potential of −1.0 V was applied for 5 min and the rods were carefully extracted. Once the construct was generated, the chamber was either immersed in the culture medium for stationary culture or connected to a syringe pump for perfusion culture. After 3 days of culture, the cells were stained with DAPI and rhodamine–phalloidin to visualize the coverage of the internal surface of the channel. After 3 days of culture, PMA was added to the culture medium at a final concentration of 20 ng/ml to accelerate spontaneous vascularization (Gamble *et al.*, 1993; Montesano and Orci, 1985). The culture was continued for an additional 14 days and luminal structures were observed using a phase-contrast fluorescent microscope (IX-71; Olympus, Japan).

3. Results and discussion

3.1. Dynamics of adsorption and desorption of the oligopeptide

A QCM was used to monitor the adsorption of the oligopeptide on a gold surface over time. The adsorption reached 95% of the final equilibrium value within 10 min (Figure 2A). This adsorption time is consistent with the results of previous studies on adsorption of alkanethiol molecules (Uosaki *et al.*, 1991; Yamada and Uosaki, 1997). The amount of adsorbed oligopeptide at 30 min was estimated to be 0.18 nmol/cm^2. This amount is sufficiently high for the adhesion of cells because typical cases require a maximum of ~20 pmol/cm^2 (Houseman

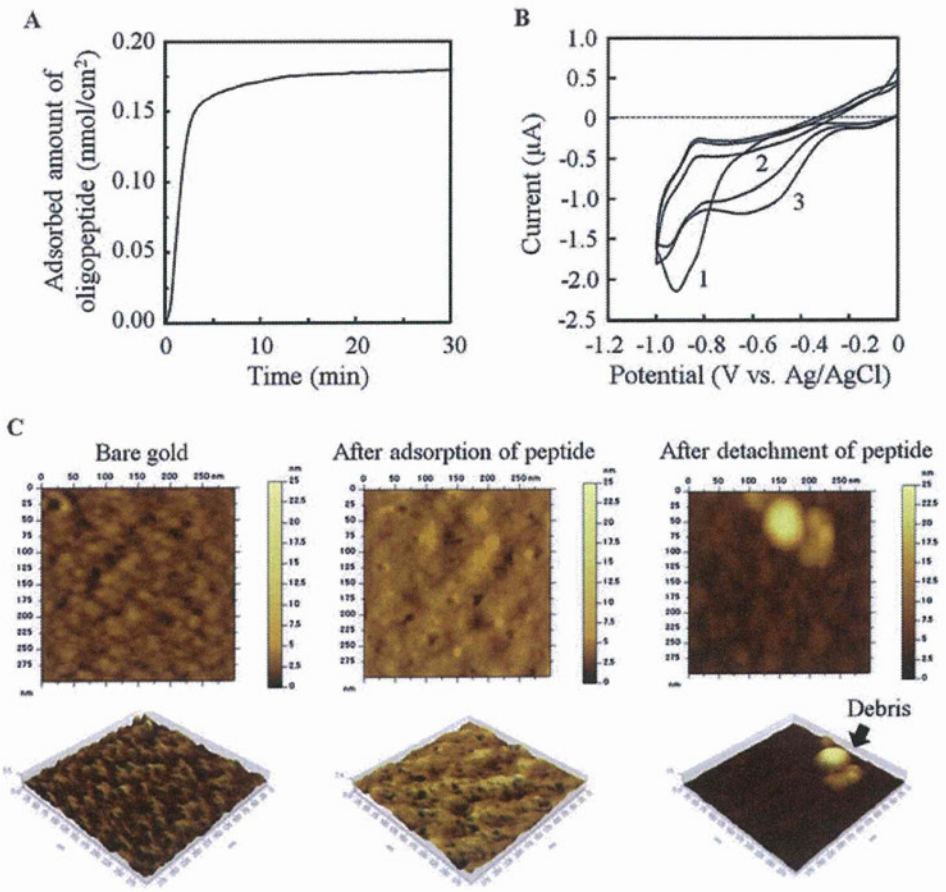

Figure 2. Dynamics of adsorption and desorption of the oligopeptide. (A) Adsorption of the oligopeptide monitored using a QCM: the adsorption reached 95% of the final equilibrium value within 10 min. (B) Cyclic voltammogram obtained during the reductive desorption of the oligopeptide. The labelled digits indicate the scan number. Cyclic voltammograms were recorded at a scanning rate of 20 mV/s with respect to a Ag/AgCl reference electrode. The working electrode area was 4.9 mm^2. (C) AFM images of the bare gold surface and the gold surface after adsorption and desorption of the oligopeptide. The bottom row shows 3D representations of each image. The scanning areas are 300 × 300 nm

and Mrksich, 2001). Meanwhile, cyclic voltammetry was used to evaluate the desorption of the oligopeptide from the gold surface. The peak potential for reductive desorption of the oligopeptide was −0.88 V in the first scan (Figure 2B). In the second and third scans, the apparent peak at −0.88 V disappeared, thus indicating that the oligopeptide was readily desorbed by the first potential scan. Broad peaks emerged in the vicinity of −0.6 V in the second and third scans. This is likely attributable to penetration of exogenous oxygen during the measurements. On the basis of the results, a potential of −1.0 V was selected for subsequent cell detachment experiments.

AFM analysis was carried out to investigate changes in surface topography after the adsorption and desorption of the oligopeptide (Figure 2C). The analysis showed that the bare gold surface was rough and irregular, with a maximal height difference of ~25 nm. This topography is probably attributable to the selection of a very thin gold layer (40 nm height) to allow cell observation by phase-contrast microscopy. A longer sputtering period and annealing processes may be required to obtain a smoother surface at the nanometer level. It is important to note that the processes of adsorption and desorption of the peptide are affected by gold substrate topography, as previously reported for thiolate coatings (Cortes *et al.*, 2009). It should also be noted that the gold layer on the QCM is thicker (250 nm height) but not treated by thermal annealing. The topography of the gold surface and its relationship to cell detachment will be our focus of attention in future investigations. After immersion in the peptide solution, the oligopeptide became spontaneously adsorbed across the entire surface with some small defects, which were visible as black portions (Figure 2C). After application of the electrical potential, the peptide was desorbed from the surface. Some debris was identified in aggregates (arrow) on the surface (Figure 2C). This appears to be a part of adsorbed oligopeptide. Further examinations will be required to clarify the details of this observation.

3.2. Detachment of single cells by electrochemistry

Fibroblasts became readily attached and were dispersed on the surface (Figure 3A). After 2 days of culture, the cells were detached on application of the potential for 5 min. The cells were gradually detached and appeared bright and round (Figure 3B). In this process, the projection area of the cells decreased to 48% and circularity increased from 0.39 to 0.67 (Figure 4A). After 5 min of application of the potential, most of the cells (82 ± 7.4%)

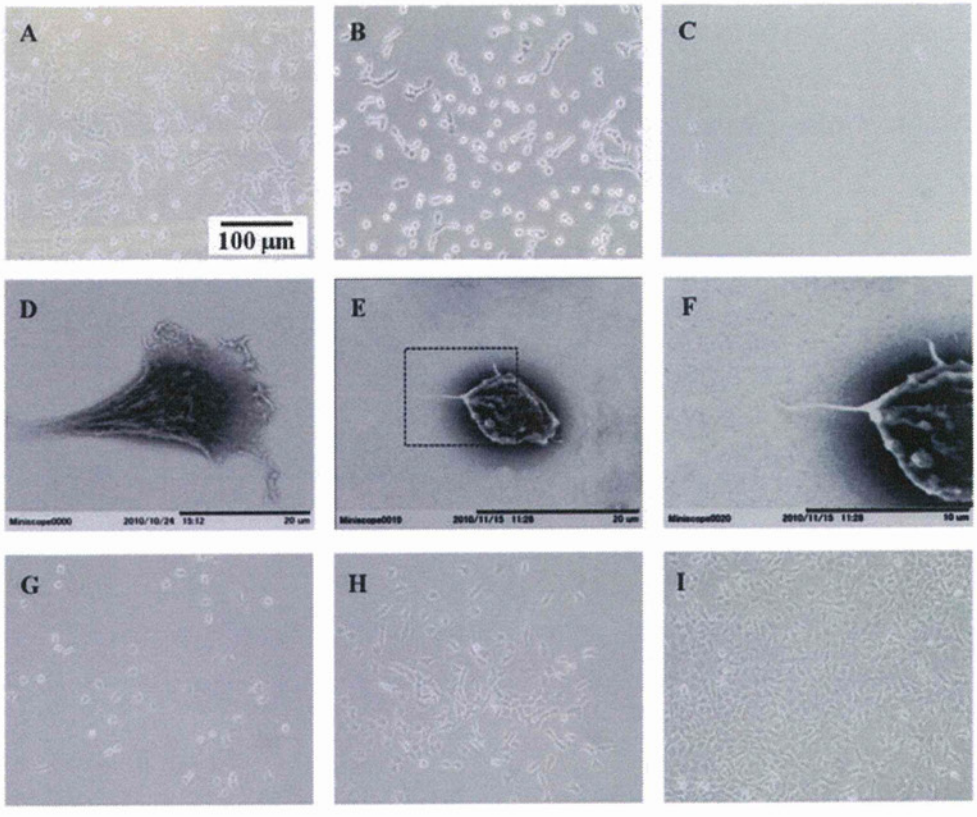

Figure 3. Fibroblasts on the gold surface modified with the oligopeptide. (A) Cells cultured for 2 days. (B) Cells after application of −1.0 V for 5 min; the cells appeared bright and round. (C) The gold surface after gentle rinsing. (D – F) SEM images of fibroblasts before (D) and after application of the potential (E). (F) A magnified view of the square in (E). (G – I) Proliferation of cells that were reseeded in a culture dish 1 (G), 2 (H) and 3 days (I) after application of the potential

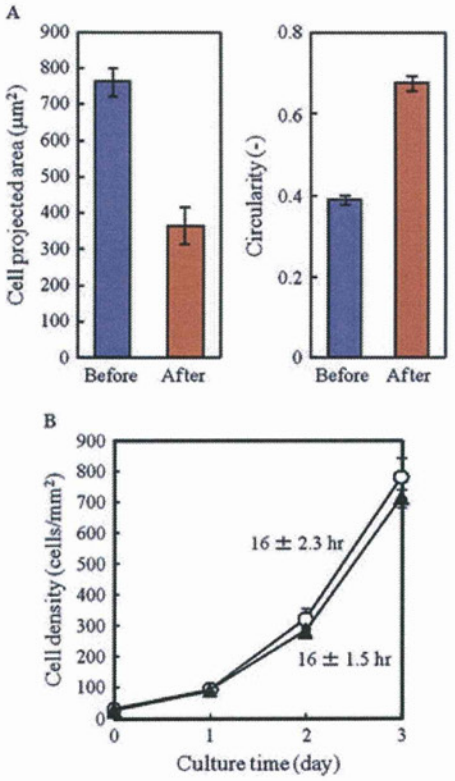

Figure 4. Quantitative characterization of cells detached by application of the potential. (A) Changes in the area and circularity of cells before and after potential application. (B) Proliferation of cells detached and reseeded on a conventional dish. White circles, electrically detached cells; black triangles, trypsinized cells; error bars, standard deviations (SDs) calculated from three independent experiments for each plot. Digits in graph indicate average doubling times after 3 days of culture

were withdrawn into a micropipette and found to be detached (Figure 3C). SEM images also indicated that fibroblasts were dispersed on the surface and appeared round after the potential was applied (Figure 3D, E). In addition, this analysis showed that the rounded cells were not completely detached and remained loosely anchored on the surface with filopodium-like structures. However, these connections were readily disrupted by gentle pipetting.

Approximately 18% of the remaining cells did not significantly detach, even when the time of application of the potential was extended to 7 min. This suggests that these cells were non-specifically adhered to the surface via adsorbed proteins or to the defective portions of the peptide coating identified in the AFM analysis. We have previously shown that fibroblasts seeded onto a gold surface modified with an alkanethiol self-assembled monolayer could be detached by the application of potential (Inaba *et al.*, 2009). In this previous study, $99 \pm 0.3\%$ of the cells were detached. Thus, the dense alkanethiol monolayer has superior characteristics in terms of cell retrieval. Recently we further demonstrated that the alkanethiol monolayer on micropatterned electrodes can be used to detach cells in succession in a spatially controlled manner with single-cell resolution (Fukuda *et al.*, 2011). However, it is important to consider that alkanethiol and similar organic chemicals may remain in the detached tissues and potentially cause inflammatory responses or other adverse reactions after transplantation of the engineered tissue. The use of oligopeptides is expected to be a promising alternative to avoid this biocompatibility issue. Indeed, this class of molecule is naturally present in the human body and can thus be metabolized to amino acids, either by means of enzymatic processes or by simple hydrolysis. To optimize the process of cell retrieval, new oligopeptide designs are now under investigation with the objective of designing dense self-assembled monolayers on a surface that would avoid unspecific protein adsorption.

To evaluate whether cell viability is affected by the electrochemical desorption process, cells were withdrawn using a pipette and transferred to a conventional culture dish, where they were subsequently cultured. These cells dispersed on the surface and proliferated (Figure 3G–I). The proliferation rate of the detached cells (doubling time, 16 ± 2.3 h) was comparable to the doubling time of a typical subculture (16 ± 1.5 h) (Figure 4B) and the doubling time reported in the literature (16.6 h) (Rossow *et al.*, 1979). These results indicate that the proposed oligopeptide and electrical detachment did not exert a significant adverse effect on the cells.

3.3. Detachment of cell sheets

Fibroblast sheets were also detached from the surface by the application of a negative potential (Figure 1B). Fibroblasts were cultured and grown to confluence for 7 days on the gold substrate with the oligopeptide. Application of -1.0 V to the surface caused detachment of a single-layered cell sheet (25×25 mm) within 10 min (Figure 5A). Live/dead fluorescent staining showed that all of the cells in the harvested cell sheet were viable, with negligible amounts of dead cells (Figure 5B). The cross-section of the cell sheet was composed of a few layered cells with close cell–cell connections (Figure 5C). As we have previously reported with alkanethiols (Inaba *et al.*, 2009), the cell sheets were easily stacked with other cell sheets in succession to form a multilayered cell sheet (data not shown). We could find only one study concerning the use of electrochemical approaches for the detachment of cell sheets. In this reported study, a polyelectrolyte layer electrostatically adsorbed on an electrode was desorbed by application of a positive potential (Guillaume-Gentil *et al.*, 2008). The desorption mechanism was considered to rely on a local pH change for subsequent dissolution of the polyelectrolyte layer. With this technique, fibroblast sheets were detached by application of $+1.8$ V for 30 min. However, this approach may have a drawback. The pH change produced by application of a potential beyond the electrical potential window of the electrode for a long period time may exert harmful effects on the cells. More recently, the same group reported a faster and less invasive approach using mesenchymal stem cells, based on the same principle (Guillaume-Gentil *et al.*, 2011). We believe that the emerging electrical cell sheet

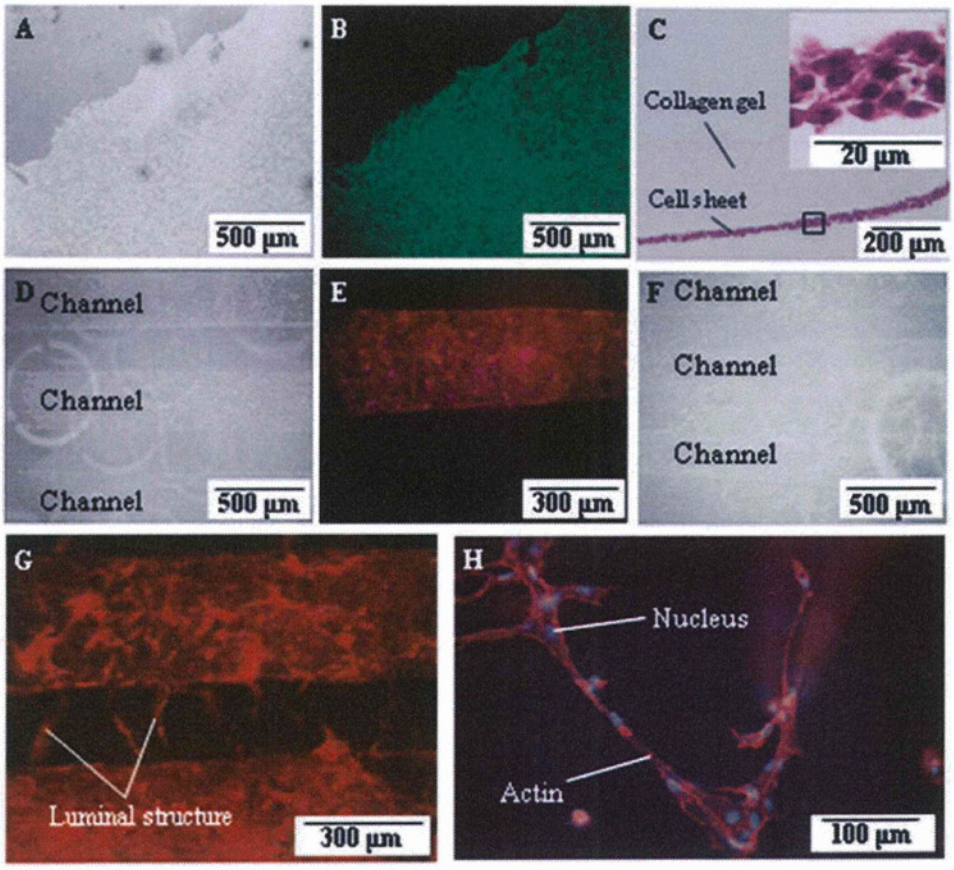

Figure 5. Detachment of cell sheets and formation of capillary-like structures. (A) Fibroblasts were grown to form a cell sheet for 7 days and were then detached by the application of electrical potential (−1.0 V for 10 min). (B) The fluorescent staining of live and dead cells shows that almost all of the fibroblasts in the sheet were viable (green) with a negligible number of dead cells (red). (C) Haematoxylin and eosin staining of the detached fibroblast sheet. Inset image shows the magnified view of the region enclosed by the square. (D) HUVECs were transferred from gold rods to the internal surface of capillary structures in a collagen gel. (E) Nucleus and F-actin staining of the HUVECs adhering to the internal surface. (F) HUVECs migrated and sprouted, and eventually formed luminal structures in the collagen gel after 17 days of culture; arrows indicate channels. (G) HUVECs stained with rhodamine–phalloidin after 7 days of perfusion culture. (H) Magnified view of luminal structures; double staining with rhodamine–phalloidin and DAPI

engineering approaches, including our proposed technology, hold great promise for future application in regenerative medicine.

3.4. Fabrication of capillary-like structures in collagen gel

One of the major obstacles in the engineering of thick tissue constructs is the need to fabricate vascular networks throughout tissues (Laschke *et al.*, 2006; Fukuda *et al.*, 2004, 2005). To address this issue, we modified our approach to fabricate capillary-like structures (Figure 1C). Rods covered with HUVECs were aligned in the chamber and a collagen solution was poured and allowed to form a gel. After application of a potential of −1.0 V for 5 min, the rods were carefully extracted from the chamber through guide holes. The cells were transferred from the gold rods to collagen, thereby creating capillary-like structures (Figure 5D). The distance between the capillaries was ~500 μm and the longitudinal length was 16 mm. The nuclei and F-actin of the cells were fluorescently stained, and the results showed that the internal surface of the capillary was densely covered with cells after 3 days of culture (Figure 5E). A culture medium was then perfused through the capillaries at a flow rate of 10 μl/min. Although the structure was initially rough and primitive, angiogenesis occurred throughout the endothelial cells on the surface. This eventually induced connections between the adjacent capillary structures in perfusion culture (Figure 5F–H). This phenomenon is an example of the well-known angiogenic process, which occurs in collagen gel. The perfusion of culture medium was not necessarily required for oxygen supply to HUVECs in this experiment. However, the introduction of a second cell population (e.g. metabolically active hepatocytes) into the collagen would require a prompt initiation of culture medium flow to satisfy oxygen and nutrient demands. This approach can potentially be used for engineering of vascularized tissue structures.

4. Conclusions

This study established a simple approach for detachment of cells from a culture surface by using electrochemical techniques. The surface was prepared by simply dipping a substrate into a solution containing an oligopeptide and did not require any reactions involving organic compounds. The oligopeptide was desorbed by application of −1.0 V for 5 min, resulting in non-invasive detachment of over 80% of adherent cells. This approach was also successfully applied to two-dimensional cell sheets and to gold-coated micro-rods to fabricate capillary-like structures, which were lined by endothelial cells in the collagen gel. During the subsequent perfusion culture, luminal structures were created from the endothelial cells, which bridged neighbouring capillaries. This technique may provide a useful tool for fabricating thicker cell sheets and vascularized tissues and organs.

Acknowledgements

This research was supported by MEXT [Grant-in-Aid for Young Scientists (A), No. 20686056], the Ministry of Health, Labour and Welfare (Grant No. H20-Saisei-wakate-010) and NEDO (Industrial Technology Research Grant Programme, Grant No. 06A06014a).

References

Atala A. 2009; Engineering organs. *Curr Opin Biotechnol* **20**: 575–592.

Cortes E, Rubert AA, Benitez G, *et al.* 2009; Enhanced stability of thiolate self-assembled monolayers (SAMs) on nanostructured gold substrates. *Langmuir* **25**: 5661–5666.

Fukuda J, Kameoka Y, Suzuki H. 2011; Spatio-temporal detachment of single cells using microarrayed transparent electrodes. *Biomaterials* **32**: 6663–6669

Fukuda J, Khademhosseini A, Yeo Y, *et al.* 2006a; Micromolding of photocrosslinkable chitosan hydrogel for spheroid microarray and co-cultures. *Biomaterials* **27**: 5259–5267.

Fukuda J, Mizumoto H, Nakazawa K, *et al.* 2004; Hepatocyte organoid culture in elliptic hollow fibers to develop a hybrid artificial liver. *Int J Artif Organs* **27**: 1091–1099.

Fukuda J, Okamura K, Ishihara K, *et al.* 2005; Differentiation effects by the combination of spheroid formation and sodium butyrate treatment in human hepatoblastoma cell line (Hep G2): a possible cell source for hybrid artificial liver. *Cell Transplant* **14**: 819–827.

Fukuda J, Sakai Y, Nakazawa K. 2006b; Novel hepatocyte culture system developed using microfabrication and collagen/polyethylene glycol microcontact printing. *Biomaterials* **27**: 1061–1070.

Gamble JR, Matthias LJ, Meyer G, *et al.* 1993; Regulation of *in vitro* capillary tube formation by anti-integrin antibodies. *J Cell Biol* **121**: 931–943.

Guillaume-Gentil O, Akiyama Y, Schuler M, *et al.* 2008; Polyelectrolyte coatings with a potential for electronic control and cell sheet engineering. *Adv Mater* **20**: 560–565.

Guillaume-Gentil O, Semenov OV, Zisch AH, *et al.* 2011; pH-controlled recovery of placenta-derived mesenchymal stem cell sheets. *Biomaterials* **32**: 4376–4384.

Houseman BT,Mrksich M. 2001; The microenvironment of immobilized Arg–Gly–Asp peptides is an important determinant of cell adhesion. *Biomaterials* **22**: 943–955.

Inaba R, Khademhosseini A, Suzuki H, *et al.* 2009; Electrochemical desorption of self-assembled monolayers for engineering cellular tissues. *Biomaterials* **30**: 3573–3579.

Kazmers NH, Ma SA, Yoshida T, *et al.* 2009; Rho GTPase signaling and PTH 3–34, but not PTH 1–34, maintain the actin cytoskeleton and antagonize bisphosphonate effects in mouse osteoblastic MC3T3-E1 cells. *Bone* **45**: 52–60.

Khademhosseini A, Bettinger C, Karp JM, *et al.* 2006; Interplay of biomaterials and microscale technologies for advancing biomedical applications. *J Biomater Sci Polym Ed* **17**: 1221–1240.

Kohane DS,Langer R. 2008; Polymeric biomaterials in tissue engineering. *Pediatr Res* **63**: 487–491.

Kwon OH, Kikuchi A, Yamato M, *et al.* 2003; Accelerated cell sheet recovery by co-grafting of PEG with PIPAAm onto porous cell culture membranes. *Biomaterials* **24**: 1223–1232.

Langer R,Vacanti JP. 1993; Tissue engineering. *Science* **260**: 920–926.

Laschke MW, Harder Y, Amon M, *et al.* 2006; Angiogenesis in tissue engineering: breathing life into constructed tissue substitutes. *Tissue Eng* **12**: 2093–2104.

Mironov V, Visconti RP, Kasyanov V, *et al.* 2009; Organ printing: tissue spheroids as building blocks. *Biomaterials* **30**: 2164–2174.

Montesano R,Orci L. 1985; Tumor-promoting phorbol esters induce angiogenesis *in vitro*. *Cell* **42**: 469–477.

Nichol JW,Khademhosseini A. 2009; Modular tissue engineering: engineering biological tissues from the bottom up. *Soft Matter* **5**: 1312–1319.

Nishida K, Yamato M, Hayashida Y, *et al.* 2004; Corneal reconstruction with tissue-engineered cell sheets composed of autologous oral mucosal epithelium. *N Engl J Med* **351**: 1187–1196.

Ohashi K, Yokoyama T, Yamato M, *et al.* 2007; Engineering functional two- and three-dimensional liver systems *in vivo* using hepatic tissue sheets. *Nat Med* **13**: 880–885.

Okano T. 2008; Cell sheet engineering for clinical application. *Tissue Eng Part A* **14**: 710–710.

Rossow PW, Riddle VG,Pardee AB. 1979; Synthesis of labile, serum-dependent protein in early G_1 controls animal cell growth. *Proc Natl Acad Sci USA* **76**: 4446–4450.

Sadr N, Zhu M, Osaki T, *et al.* 2011; SAM-based cell transfer to photopatterned hydrogels for microengineering vascular-like structures. *Biomaterials* **32**: 7479–7490.

Seto Y, Inaba R, Okuyama T, *et al.* 2010; Engineering of capillary-like structures in tissue constructs by electrochemical detachment of cells. *Biomaterials* **31**: 2209–2215.

Sung HJ, Meredith C, Johnson C, *et al.* 2004; The effect of scaffold degradation rate on three-dimensional cell growth and angiogenesis. *Biomaterials* **25**: 5735–5742.

Tekin H, Anaya M, Brigham MD, *et al.* 2010; Stimuli-responsive microwells for formation and retrieval of cell aggregates. *Lab Chip* **10**: 2411–2418.

Uosaki K, Sato Y,Kita H. 1991; Electrochemical characteristics of a gold electrode modified with a self-assembled monolayer of ferrocenylalkanethiols. *Langmuir* **7**: 1510–1514.

Yamada R, Uosaki K. 1997; *In situ*, real-time monitoring of the self-assembly process of decanethiol on Au(111) in liquid phase. A scanning tunneling microscopy investigation. *Langmuir* **13**: 5218–5221.

TISSUE ENGINEERING: Part A
Volume 19, Numbers 1 and 2, 2013

DOI: 10.1089/ten.tea.2011.0739

Cell-Adhesive and Cell-Repulsive Zwitterionic Oligopeptides for Micropatterning and Rapid Electrochemical Detachment of Cells

Takahiro Kakegawa, M.S.,[1] Naoto Mochizuki, M.S.,[1] Nasser Sadr, Ph.D.,[2] Hiroaki Suzuki, Ph.D.,[1] and Junji Fukuda, Ph.D.[1]

In this study, we describe the development of oligopeptide-modified cell culture surfaces from which adherent cells can be rapidly detached by application of an electrical stimulus. An oligopeptide, CGGGKEKEKEK, was designed with a terminal cysteine residue to mediate binding to a gold surface via a gold–thiolate bond. The peptide forms a self-assembled monolayer through the electrostatic force between the sequence of alternating charged glutamic acid (E) and lysine (K) residues. The dense and electrically neutral oligopeptide zwitterionic layer of the modified surface was resistant to nonspecific adsorption of proteins and adhesion of cells, while the surface was altered to cell adhesive by the addition of a second oligopeptide (CGGGKEKEKEKGRGDSP) containing the RGD cell adhesion motif. Application of a negative electrical potential to this gold surface cleaved the gold–thiolate bond, leading to desorption of the oligopeptide layer, and rapid (within 2 min) detachment of virtually all cells. This approach was applicable not only to detachment of cell sheets but also for transfer of cell micropatterns to a hydrogel. This electrochemical approach of cell detachment may be a useful tool for tissue-engineering applications.

Introduction

The spatial and temporal control of the biointerface between adherent cells and materials remains an important challenge in biomaterial science.[1] The ability to dynamically control the cell adhesive properties of a substrate has recently been shown to be a powerful tool that may foster advances in diverse fields, ranging from cell biology to tissue engineering.[2] Early and excellent examples of manipulation of attachment and detachment of cell layers were reported using a thermally responsive polymer, poly(N-isopropylacrylamide).[3] Several types of cell sheets, including those composed of myocardial and hepatic cells, were noninvasively detached from thermally responsive surfaces and stacked to form multilayered cell sheets.[4,5] Clinical results using this thermoresponsive technology have shown that reconstructed corneal tissues remain clear and mediate improved visual acuity over 1-year follow-up after transplantation of corneal epithelial cell sheets.[6] However, one potential drawback to this approach could be that the harvesting of cells typically requires 40–60 min at a low temperature.[7,8] Promising alternative approaches have been reported using electrochemically responsive surfaces. For instance, quinone ester and O-silyl hydroquinone electroactive groups have been used to selectively release cell adhesive ligands, and thus the adherent cells, in response to application of reductive or oxidative potentials.[9] Similarly, application of an electrical stimulus to electrodes coated with hydrogels and polyelectrolyte layers has also been used to detach adherent cells.[10,11] One promising feature of such electrochemical approaches is that cells can be detached not only from a flat surface but also from substrates of varying configuration, such as microarrayed electrodes for spatially controlled single-cell detachment[12] and cylindrical rods for fabricating three-dimensional vascular-like structures.[13,14]

To date, our group has used two different molecular supports for electrochemically detaching cells from a surface. In the first approach, an alkanethiol self-assembled monolayer (SAM) was formed on a gold electrode, and the alkanethiol carboxyterminals were coupled to RGD peptides to mediate cell adhesion.[15] The second approach employed a custom-designed bridge-shaped oligopeptide, CCRRGDWLC, which spontaneously adsorbed onto the gold surface via the terminal cysteines and mediated cell adhesion through the central RGD sequence.[13,16] In both approaches, the molecules adsorbed to the gold surface via formation of a gold–thiolate bond. This bond can be reductively cleaved by applying a negative electrical potential,

[1]Graduate School of Pure and Applied Sciences, University of Tsukuba, Ibaraki, Japan.
[2]Cell and Tissue Engineering Laboratory, IRCCS Istituto Ortopedico Galeazzi, Milan, Italy.

thereby detaching adherent cells along with desorption of the molecules. Our results demonstrated that cells and cell sheets could be rapidly harvested from the gold surface using both these approaches. Indeed, the alkanethiol SAM-based approach allowed almost 100% cell retrieval after application of a negative potential for only 5 min. In this case, however, the detached cells may retain the alkanethiol molecules. In previous studies, alkanethiol SAM-coated surfaces have been shown to cause local acute inflammatory reactions and adhesion of leukocytes *in vivo*.[17,18] It is possible that alkanethiol molecules transferred with the cells induce the inflammatory reaction, which would compromise the biocompatibility of this approach. Furthermore, chemical agents used to couple RGD peptides to the carboxyterminals of alkanethiol SAMs could also be a source of toxic contaminants. The use of oligopeptides represents a promising alternative to overcome the problem of biocompatibility for the use in humans; peptides are naturally occurring molecules, and there are many enzymatic routes for their degradation *in vivo*. In addition, the chemistry to generate peptide–SAMs does not require additional potentially toxic substances. However, in our previous studies, using the bridge-shaped oligopeptide, we found that ~10% of cells remained attached on the surface even after 7 min of potential application. The efficient cell detachment using the alkanethiol SAM is likely due to this molecule's ability to form a dense molecular layer on the gold surface, preventing nonspecific protein adsorption. In contrast, the amino acid sequence of the bridge-shaped oligopeptide was not optimized for generation of compact layers, and most likely allowed some nonspecific protein adsorption that impaired cell detachment. In the present study, we hypothesized that such limitations in cell detachment could be overcome by designing an oligopeptide SAM that forms a dense layer on the gold surface. Thus, we aimed to design novel oligopeptides that would allow rapid and reliable electrochemical desorption for cell retrieval, whereas avoiding the biocompatibility concerns inherent to the alkanethiol-based approaches.

To fulfill this aim, we prepared two zwitterionic oligopeptides that promote dense monolayer formation by exploiting intermolecular electrostatic forces (Fig. 1). We characterized the modified surface in terms of molecular density and inhibition of nonspecific protein adsorption, and additionally evaluated the ability of the oligopeptides to support efficient and rapid cell detachment upon electrical potential application. Finally, we explored the potential for this approach to be exploited as a tool for manipulating cell sheets and cell micropatterns for tissue engineering *in vitro*.

Materials and Methods

Materials and reagents

Swiss 3T3 murine fibroblasts (RCB1642) were purchased from the Riken Cell Bank, Japan. Human umbilical vein endothelial cells constitutively expressing green fluorescent protein (GFP-HUVEC) were a generous gift from Dr. J. Folkman (Children's Hospital Boston). Endothelial basal medium-2 (EBM-2, CC-3156) and SingleQuots growth supplement (CC-3162) were purchased from Cambrex Bio Science. Human bone marrow-derived mesenchymal stem cells (hBMSCs) were purchased from Lonza. Cell culture reagents were purchased from the following commercial sources: Dulbecco's modified Eagle's medium (DMEM), fetal bovine serum (FBS), and phosphate-buffered saline (PBS) from Invitrogen; type I collagen solution from Nitta Gelatin; fibronectin and fibrinogen from Sigma; fluorescein diacetate (FDA) and ethidium bromide (EB) from Wako Pure Chemicals Industries.

The materials for the fabrication of culture substrates were as follows: microcover glass (24×24 mm) from Matsunami; a thick-film photoresist (SU-8) from MicroChem; poly(dimethylsiloxane) (PDMS) from ShinEtsu Chemical; cell-repulsive oligopeptide, CGGGKEKEKEK (Fig. 1A), cell-adhesive oligopeptide, CGGGKEKEKEKGRGDSP (Fig. 1B), and bridge-shaped oligopeptide, CCRRGDWLC,[13] from Sigma-Aldrich.

Gold surface modification with oligopeptides and assessment of nonfouling properties

A quartz crystal microbalance (QCM, AFFINIX QN; Initium) was used to quantify adsorption of the cell-repulsive oligopeptide (Fig. 1C) or the bridge-shaped oligopeptide on the gold surface, and to estimate the nonfouling properties of the oligopeptide-modified surfaces after protein adsorption. QCM gold electrodes were cleaned with 1% sodium dodecyl sulfate and a piranha solution (H_2SO_4:H_2O_2, 3:1), then rinsed with double distilled water (ddH_2O; Milli-Q Advantage; Millipore), and dried under N_2. The electrodes were immersed in a 50-μM solution of cell-repulsive or bridge-shaped oligopeptides for 1 h at room temperature, and then rinsed with ddH_2O and dried. The adsorbed oligopeptide was quantified by the change in the resonance frequency calculated using the Sauerbrey equation. The modified electrodes were then immersed in a 1.0 mg/mL aqueous solution of fibronectin or fibrinogen for 30 min at room temperature. After washing with ddH_2O and drying with N_2, the adsorbed protein was again quantified by the change in the resonance frequency. An unmodified gold electrode was used as a reference surface.

Cell adhesion on oligopeptide-modified gold surfaces

Gold surfaces were prepared by sputter coating a chromium layer and an ~40-nm gold layer on microcover glasses using a sputtering machine (CFS-4ES; Shibaura). The gold-coated substrates were modified by overnight immersion at 4°C in a series of 50-μM solutions containing varying amounts of the two oligopeptides (Fig. 1D). The molar ratio of cell-adhesive to cell-repulsive oligopeptides (Fig. 1A, B) in the solutions was 100:0, 99:1, 99.9:0.1, 99.99:0.01, 99.999:0.001, and 0:100 (total concentration: 50 μM). To prepare these solutions, 0.2 mL of a 50-μM solution of the cell-adhesive oligopeptide was mixed with 1.8 mL of a 50-μM solution of the cell-repulsive oligopeptide. Subsequently, 0.2 mL of this solution was mixed with 1.8 mL of a 100% cell-repulsive oligopeptide solution to obtain a solution of 99:1 cell-repulsive to cell-adhesive oligopeptide. This procedure was repeated sequentially to generate solutions with ratios of 99.9:0.1, 99.99:0.01, and 99.999:0.001 cell-repulsive to cell-adhesive oligopeptide. The modified substrates were then rinsed with ddH_2O, followed by 70% ethanol, and were placed in wells of a six-well plate. Fibroblasts were seeded at a density of 5×10^5 cells/mL in 2 mL/well in the DMEM

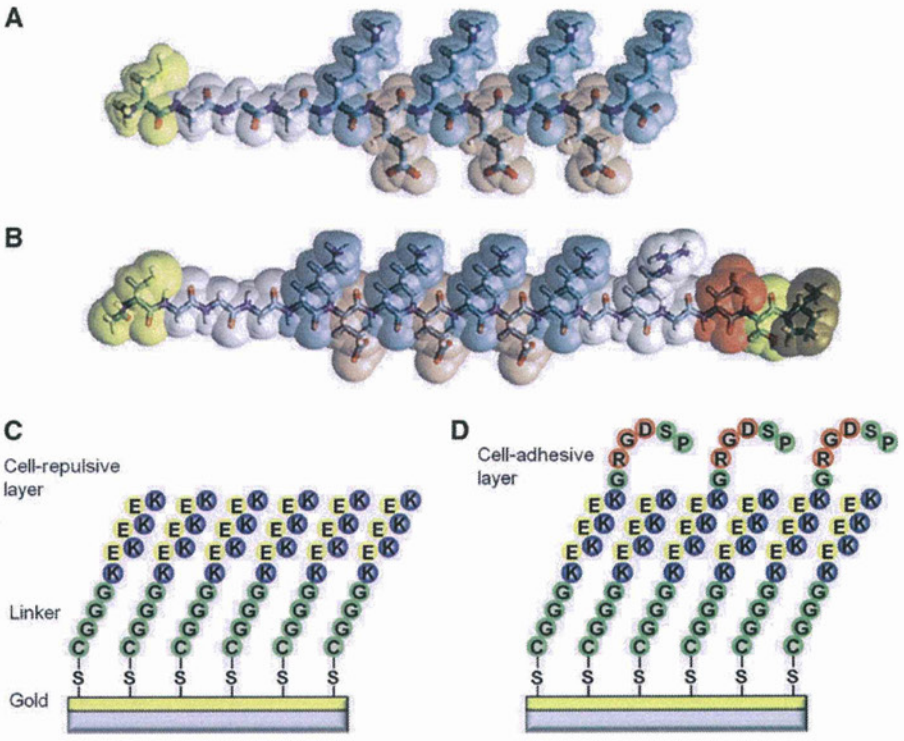

FIG. 1. Design of zwitterionic oligopeptides. **(A)** Cell-repulsive oligopeptide, CGGGKEKEKEK. **(B)** Cell-adhesive oligopeptide, CGGGKEKEKEKGRGDSP. Yellow, cysteine; white, glycine; blue, lysine; and red, glutamic acid. Both oligopeptides contain a terminal cysteine C that mediates binding to the gold surface through a gold–thiolate bond. Oligopeptides also contain a linker of three glycines G and an alternating positively charged lysine K and negatively charged glutamic acid E residues. K and E support formation of a dense self-assembled monolayer (SAM) through electrostatic forces. **(C)** SAM of the cell-repulsive oligopeptide. **(D)** SAM of the mixture of cell-adhesive and cell-repulsive oligopeptide. Color images available online at www.liebertpub.com/tea

supplemented with 10% FBS. Plates were incubated in a humidified 5% CO_2 incubator for 3 h at 37°C, after which nonadherent cells were removed by gently rinsing with PBS.[15] Phase-contrast images were acquired, and the number of adherent cells was quantified using image analysis software (Nano Hunter NS2K-Pro; Nanosystem Corp.). Growth of cells on the oligopeptide-modified substrates was also examined over 4 days in culture. To do this, fibroblasts were seeded on the modified substrates at a lower cell density (5×10^4 cells/mL in 2 mL/well), and phase-contrast images were taken to quantify the adherent cells after culture for 3 h, 1 day, 2 days, 3 days, and 4 days.

Electrochemical detachment of cells

We employed cyclic voltammetry to determine the potential required for reductive desorption of the oligopeptides from the modified gold surfaces. For this experiment, an electrolyte solution containing 0.5 M KOH was deoxygenated by bubbling with N_2 gas for 20 min immediately before the measurement. The deoxygenation step is required to eliminate the interfering current generated by reduction of oxygen. The gold substrate was modified by immersion in a 50-μM solution of cell-adhesive oligopeptide overnight at 4°C. The oligopeptide-modified gold electrode, an Ag/AgCl reference electrode (#2080 A; Horiba), and a platinum auxiliary electrode were then placed in the electrolyte solution and connected to an electrochemical measurement system (AUTOLAB; Metrohm Autolab). A cyclic voltammogram was recorded at a scanning rate of 20 mV/s from 0 to −1.0 V. In this study, all potential values refer to those measured with respect to the Ag/AgCl electrode.

To examine cell detachment, fibroblasts were seeded on the modified substrates (2.5×10^5 cells/mL, 2 mL/well) and cultured as described above. After 1 day of culture, the substrates were rinsed three times with PBS and immersed in PBS with an Ag/AgCl reference electrode and a platinum auxiliary electrode. The substrate and electrodes were then connected to a potentiostat (HA-151; Hokuto Denko), and −1.0 V was applied for 1, 2, or 3 min. The substrates were then removed, gently rinsed, and phase-contrast micrographs were taken to quantify the adherent cells. Control substrates included unmodified gold surfaces or surfaces modified with the bridge-shaped oligopeptide or 10-carboxy-1-decanethiol.

Electrochemical detachment of cell sheets

We also examined whether this detachment method could be used for cell sheets in addition to single cells. For these experiments, hBMSCs were suspended at 5×10^5 cells/mL in the DMEM supplemented with 10% FBS, and 2 mL was seeded onto the modified or control substrates and placed in a 35-mm dish. Cells were cultured for 3 days until they reached confluence on the substrate. A collagen solution (2.4 mg/mL in 10×Ham's F12 medium, 0.05 N NaOH, 200 mM HEPES, and 2.2% [wt/v] $NaHCO_3$) was freshly prepared, and a few drops were poured onto the confluent cell sheet and then allowed to gel. A potential of −1.0 V was applied for 5 min, and the gel layer was peeled from the substrate surface. The viability of detached cells was evaluated using a live/dead fluorometric assay using FDA and EB.[19] Viable cells were identified by the green cytoplasmic fluorescence of FDA, whereas the dead cells showed red nuclear fluorescence due to binding of EB.